R. & M. No. 3808

R. & M. No. 3808


PROCUREMENT EXECUTIVE, MINISTRY OF DEFENCE

AERONAUTICAL RESEARCH COUNCIL

REPORTS AND MEMORANDA

# A Pyramid Skewed Axis Sensor Set for Multiplex Flight Control Systems

BY D. KIMBERLEY

Flight Systems Dept., R.A.E., Farnborough, Hants.



LONDON: HER MAJESTY'S STATIONERY OFFICE

1978

£4 net

# A Pyramid Skewed Axis Sensor Set for Multiplex Flight Control Systems

By D. Kimberley

Flight Systems Dept., R.A.E., Farnborough, Hants.

*Reports and Memoranda No.* 3808*

*July*, 1975

**Summary**

In order to meet the 'two defect survival' capability in future full-time flight control systems, one approach is to use four identical sensors in each axis, giving a total of twelve for a three-axis system. An alternative eight Sensor Pyramid Arrangement has been developed which offers a similar 'two defect survival' capability in all three axes leading to reduced cost and maintenance effort but with slightly larger transients following failure of a sensor. The pyramid arrangement can also be used for 'fail safe' systems reducing the number of sensors from six to four, or alternatively for a twelve gyro, 'four defect survival' configuration.

* Replaces R.A.E. TR 75055-A.R.C. 36 355

LIST OF CONTENTS

Appendix C Eight Gyro Pyramid Set B Failure Transients

Table 1

Tables 2 and 3

Illustrations Figs. 1 to 9

## 1. Introduction

The safety requirement[1] demanded of 'full time fly-by-wire' flight control systems, i.e. systems whose failure causes loss of control of the aircraft, is that the system failure rate must be less than one failure per $10^7$–$10^8$ flying hours. The predicted defect rates of the various system components are such that this requirement can be met if the overall system continues to function correctly after any two defects have occurred, i.e. a 'two defect survival' system. Design studies for such systems have proposed quadruplex solutions (Fig. 1) in which four lanes of control are used in each axis to provide the 'two defect survival' capability.

Most of the flight control systems under consideration use single degree of freedom sensors (e.g. rate gyroscopes) installed with their sensitive axes along one of the aircraft's axes of control. Thus, for a quadruplex system providing control in three axes (pitch, roll and yaw), twelve sensors are used. These are arranged as in Fig. 2, each set of four sensors having its input axis parallel to one of the aircraft's axes. Using this Twelve Sensor Orthogonal Arrangement it is possible to produce a system in which the control lanes are completely isolated[2] (i.e. no signal crossfeeds between lanes). Systems of this form impose severe constraints upon the computational accuracy and the operating tolerances of the system components if unacceptable transients are not to occur at the aircraft's control surface whenever a component fails. These constraints can be relaxed by incorporating signal consolidation processes whereby the cross-transfer of information between control lanes allows each lane to operate with the same 'best' estimate. The consolidation process may occur several times within a system but the majority of proposed systems include consolidation of the sensor output signals. Thus for the system shown in Fig. 1 crossfeeds are introduced[3] so that each lane receives information from all twelve sensors. This is shown in Fig. 3, the data highways implying transfer of sensor signals between the four computers.

Detailed studies are currently being made to ensure that the cross-transfer of sensor information can be performed to the required integrity. This introduces the possibility of reducing the number of single degree of freedom sensors used, thus reducing the system first time cost and also the amount of maintenance effort required. In this Report this possibility is discussed and a detailed analysis presented of a particular sensor arrangement that reduces the number of sensors from twelve to eight without increasing significantly the transient response following failures of any two sensors.

It can be shown[4] that by skewing the sensor input axes so that components of motion about more than one aircraft axis are measured, the use of six sensors will meet the 'two defect survival' requirement for all three axes. Superficial consideration could suggest that only five such sensors are necessary since the loss of two would still leave three functioning correctly to provide the required three axes information. This would be true provided that none of the original set of five are orthogonal to any other in the set. The requirement for the sixth sensor stems from the need to 'survive' a failure. This automatically implies the ability to decide which sensor has failed; such a decision can only be taken if there is additional information regarding the sensor or by majority voting. In the absence of any additional information (normally only available if the sensor has a few obvious failure modes) the majority vote approach requires six sensors so that, at the instant the second sensor fails, more estimates of vehicle motion exist based upon correctly functioning sensors than estimates containing the failed sensor. Unfortunately, analysis of one such arrangement with six gyros mounted as in Fig. 4 has shown that higher quality sensors must be used if the transient that can occur at the control surface when a sensor fails is not to be several times larger than the twelve sensor Orthogonal Arrangement, an unacceptable situation.

The Eight Sensor Pyramid Arrangement discussed in this paper overcomes this deficiency and offers other system advantages. The eight sensors are aligned in four parallel pairs, the input axis of each pair being parallel to one of the edges of a pyramid (Fig. 5). Amalgamation of the eight sensor outputs allows the 'two defect survival' requirement to be met in each of the aircraft's control axes but additional algorithms must be used to transform the sensor information from the pyramidal axes into the orthogonal aircraft axes. The amalgamation process consists of a set of consolidation algorithms which form the output to be used from the sensor inputs, and a set of error detection algorithms which are used to detect and isolate failed sensors. As with most systems many alternative algorithm sets can be formulated. Three sets of algorithms are described in this paper; with Set A there is a minimal change to the algorithms used for a Twelve Sensor Orthogonal Arrangement; with Set B the failure transients of Set A are reduced by using a novel dual set of error detection algorithms whilst Set C has been developed from Set B to provide a self-detecting battle damage capability. These sets are not considered to be 'optimum' from any particular viewpoint but have been chosen to illustrate certain attributes of the pyramid arrangement.

To simplify the discussion all systems are described as rate gyroscope sensor packages but the technique could equally be applied to other single degree of freedom sensors such as gravity compensated accelerometers.

### 1.1. Notation

Throughout this Report post-subscripts relate to a particular sensor, i.e. $\omega_i$ and $E_i$ are the $i$th gyro output and error detector respectively. Pre-subscripts always indicate the gyros which have failed and been disconnected, i.e. ${}_jE_i$ is the $i$th gyro error detector following a disconnection of $\omega_j$ and ${}_jp_i$, ${}_jq_i$ and ${}_jr_i$ are the consolidated outputs for roll, pitch and yaw following an $\omega_j$ disconnection. Similarly ${}_{jk}p$, ${}_{jk}q$ and ${}_{jk}r$ are the consolidated outputs following disconnection of $\omega_j$ and then $\omega_k$.

## 2. Sensor Package General Design Requirements

Before presenting an analysis of the Twelve Gyro Orthogonal Arrangement in Section 3 and that for the proposed Eight Gyro Pyramid Arrangement in Sections 4, 5 and 6, it was considered appropriate to discuss in general terms those design factors that are affected by the choice of sensor configuration. These are discussed under the following headings:

(a) The transient response of the consolidated output when a gyro fails.
(b) The probability of system failure due to several gyro failures.
(c) The arrangement of multiplex power supplies to the gyros and the interface with the system computers.
(d) The problem of battle damage.

### 2.1. Failure Transients

The concept of using more than one lane of information to provide a defect survival capability implies that the system output will be derived by some algorithm from the various estimates (of the same quantity). Also implied is some decision process whereby a failed channel will be identified and appropriate disconnect action taken. Normally, correct fault identification can only be guaranteed under single defect circumstances, and in this paper, unless otherwise stated, only one unidentified sensor failure is considered to be present in the system at any one time.

Under ideal conditions detection and disconnection of a failed sensor would be instantaneous with negligible effect upon the consolidated output. In practice a transient is likely to be experienced since the error detection process must allow for errors in the outputs of correctly functioning gyros due to normal tolerancing effects. Additionally, when a failure has been identified it is necessary, in general, to modify the consolidation algorithm since in most cases the form of this algorithm will not inhibit the effect of the failed gyro's output. The 'switch-over' from one algorithm to another can also cause a transient so that, in general, failure transients will have two characteristic parts, a 'pre-detection transient' and a 'switch-over' transient.

*2.1.1. The pre-detection transient.* The pre-detection transient is the change in consolidated output attributable to the erroneous signal from a failed gyro prior to the decision to disconnect it. Each gyro will have a range of output values, for a given input rate, within which it is assumed to be functioning correctly. Consequently it is possible for the error in a gyro output to change from one end of the tolerance band to the other without a failure indication occurring. Disconnection at this position implies perfect error detection algorithms and it is often necessary to allow the erroneous output of a failed gyro to travel much further before correct identification of the failure can be ensured.

The magnitude of the pre-detection transient will depend not only upon the consolidation algorithm and the error detection algorithm but also upon the initial tolerances of all the gyros and the particular form of gyro failure. An example is shown in Fig. 6 where the consolidated output is the average of four gyros. After disconnection of the failed gyro the average of the remaining three gyros is used as the consolidated output. In this example, a perfect error detection algorithm has been assumed.

*2.1.2. The switch-over transient.* The failure of any gyro whose individual output forms part of the consolidated output will necessitate a change in the output algorithm. The 'switch-over' transient is caused by any differences between the values produced by the output algorithms and will generally be a rapid change from one level to the other. This transient is also a function of the consolidation and error detection

algorithms but is independent of the form of the failure since normally a switch-over decision will be taken instantaneously, irrespective of the manner in which the gyro fails.

Fig. 6 continues the example of the 'pre-detection' transient described in Section 2.1.1. to illustrate a 'switch-over' transient.

*2.1.3. The possibility of transient suppression.* The characteristic shape of the failure transient can be modified by developing consolidation algorithms which retain a memory of the output prior to disconnection of the failed gyro. If implemented perfectly this would produce a transient of the form shown in Fig. 7a, where the stored output is gradually leaked away. For 'slow' failures this would provide a very smooth transition from one output level to another but for 'rapid' gyro failures it could produce a more unacceptable situation since the 'pre-detection' transient is generally larger than, and of opposite sign to, the 'switch-over' transient. An illustration of this effect is shown in Fig. 7b.

*2.1.4. 'Maximum' and 'minimum' failure transients.* To allow comparative assessments to be made it has been assumed throughout this paper that the output of a correctly functioning gyro will always be within a tolerance $\pm\delta G$ of the true input rate. Upon failure, it is assumed that the error in the failed gyro's output changes in a consistent direction. The effect of this form of failure is described as the 'maximum failure transient'. In practice, a larger transient can occur if a gyro fails in an oscillatory manner such that its output almost causes disconnection at one limit, changes direction and then exceeds the other disconnection limit. This form of failure is most improbable and for the purposes of comparison has not been considered in this paper.

The 'minimum failure transient' is defined as the smallest transient that can occur when a gyro, with any initial error within the tolerance band $\pm\delta G$, fails such that the erroneous output changes in any consistent direction.

*2.1.5. Disconnection thresholds.* Generally there will be an error detection threshold associated with all error detection algorithms. This has an important effect upon the total system performance since if this threshold is set too high the failure transient will be unacceptably large; if set too low, sensors may be disconnected although they are still functioning correctly (the so called 'nuisance disconnect') thus increasing the probability of total system failure.

Throughout the analysis described in this Report it has been assumed that when a gyro fails the error in its output increases with time at a sufficiently fast rate for the detection thresholds to be exceeded before a second gyro fails. This assumption may, under certain circumstances be invalid. For example if a gyro fails such that its output is zero the error detection thresholds will only be exceeded if the aircraft motion is sufficiently disturbed. If the aircraft flies in an undisturbed state for a considerable length of time such a failure could be dormant within the system such that a second similar failure might cause loss of control. This problem is not considered further in this paper since it is common to all multiplex configurations, but it is essential that this problem is considered when selecting the sensors for multiplex flight control systems.

### 2.2. System Failure Probability

The reduction in the number of sensors in a system should lead to a comparable reduction in maintenance effort, e.g. a reduction in the frequency of replacing defective gyros. System safety is however related to the degree of redundancy incorporated into the system thus reduction in the number of sensors, giving a lower overall redundancy, will increase the probability of loss of control. The loss of control in a particular axis is not necessarily catastrophic, for example sufficient directional control using ailerons may remain after loss of the rudder; additional 'defect survival capabilities' of this form are dependent upon the particular airframe and the motivators controlled by the fly-by-wire system. However for the purpose of a comparison of the failure probabilities of the various sensor configurations it has been assumed that loss of control in any axis will be catastrophic. Also it is assumed that all sensor failures are completely independent. The probabilities calculated are for sensor defects only, power supply failures, computing defects etc. have been ignored.

### 2.3. Interface with Power Supplies and System Computers

More complex power supply arrangements or a more complex interface between the sensors and the system computers could result from the use of different sensor arrangements. For the discussion of the various interfaces a quadruplex system of the form shown in Fig. 3 has been assumed in which four independent power supplies and four separate lane computers are used. It has also been assumed that the

crossfeeds between computers will be used to transfer gyro information so avoiding the complexity of directly feeding every gyro output to every computer.

The interfaces are assessed in the presence of the following sets of two defects:

(a) loss of two independent power supplies.

(b) Loss of two lane computers.

### 2.4. Battle Damage

In any military aircraft, consideration must be given to the possible effects of battle damage. The criterion[1] assumed in this paper is that a single shell hit should be survived, assuming that all system components are functioning correctly prior to the shell hit.

As far as the sensors are concerned this requirement can be met by using 'armour plating', by mounting the sensors in a location which, if hit by a shell would be catastrophic for other reasons, e.g. close to the pilot, or alternatively by dispersing the sensors around the airframe. Some of the systems described later are compatible with separate installation locations but further work is necessary to investigate the effects of dispersed locations for sensors, particularly in terms of structural effects, e.g. undesirable pick up of structural modes.

## 3. The Twelve Gyro Orthogonal Arrangement

The straightforward approach to the provision of a two defect survival sensor package is to align four gyros parallel to each of the aircraft axes. Thus twelve gyros in total are used mounted in three orthogonal sets of four (Fig. 2). Each set is then 'independent' of the others and it is sufficient to consider one axis only, the roll axis being chosen for the analysis described. Thus in this section only four roll rate gyroscopes are considered, their outputs being $\omega_1$, $\omega_2$, $\omega_3$ and $\omega_4$ deg/s.

As mentioned earlier many algorithms exist both for the consolidation and the failure detection processes. It is not the intention of this paper to consider the relative merits of the various algorithms that could be used for the Twelve Gyro Orthogonal Arrangement but so that a comparison can be made with the pyramid system it is necessary to select a particular set of algorithms as a base line. The set chosen is one which produces the smallest 'maximum' failure transient for the assumptions discussed in Section 2.

### 3.1. Consolidation Algorithms

The algorithm chosen as a base line is that in which the outputs of the correctly functioning roll rate gyros are averaged to provide a consolidated output. Thus with four gyros functioning correctly the output is

$$p = \tfrac{1}{4}(\omega_1 + \omega_2 + \omega_3 + \omega_4). \tag{1}$$

After the failure of any gyro, say $\omega_1$,

$$_1p = \tfrac{1}{3}(\omega_2 + \omega_3 + \omega_4) \tag{2}$$

(the pre-subscript 1 indicating failure of gyro 1).

Similarly after a second failure, say $\omega_2$,

$$_{12}p = \tfrac{1}{2}(\omega_3 + \omega_4) \tag{3}$$

(the pre-subscript 12 indicating failure of gyro 1 followed by failure of gyro 2).

A third failure in the same axis causes loss of control in that axis.

### 3.2. Error Detection Algorithms

The form of the error detection algorithms used as a base line is that of a comparison of each gyro with the current consolidated output. Hence, when all four gyros are functioning correctly four error equations exist, one for each gyro given by:

$$E_1 = \omega_1 - p = \tfrac{1}{4}(3\omega_1 - \omega_2 - \omega_3 - \omega_4) \tag{4}$$

$$E_2 = \omega_2 - p = \tfrac{1}{4}(3\omega_2 - \omega_1 - \omega_3 - \omega_4) \tag{5}$$

$$E_3 = \omega_3 - p = \tfrac{1}{4}(3\omega_3 - \omega_1 - \omega_2 - \omega_4) \tag{6}$$

$$E_4 = \omega_4 - p = \tfrac{1}{4}(3\omega_4 - \omega_1 - \omega_2 - \omega_3) \tag{7}$$

A failure is detected whenever the magnitude of one of the $E$'s exceeds a threshold $T_a$.

After a failure of a gyro, say $\omega_1$, another set of algorithms are used:

$$ {}_1E_2 = \omega_2 - {}_1p = \tfrac{1}{3}(2\omega_2 - \omega_3 - \omega_4) \tag{8} $$

$$ {}_1E_3 = \omega_3 - {}_1p = \tfrac{1}{3}(2\omega_3 - \omega_2 - \omega_4) \tag{9} $$

$$ {}_1E_4 = \omega_4 - {}_1p = \tfrac{1}{3}(2\omega_4 - \omega_2 - \omega_3) \tag{10} $$

a failure being detected whenever the magnitude of one of the $E$'s exceeds a threshold $T_b$.

Another set can be generated following a second failure (e.g. ${}_{12}E_3 = \omega_3 - {}_{12}p$) but these can only indicate that a third failure has occurred, they cannot correctly identify which of the remaining two gyros has failed.

*3.2.1. Error Detection Thresholds.* To complete the error detection algorithms it is necessary to define $T_a$ and $T_b$.

Inspection of the error detectors (equations (4) to (7)) shows that, upon failure of any gyro such that its output changes, the magnitude of all of the $E_i$ will also change since each equation contains the failed gyro's output. Hence it is essential that the threshold $T_a$ is chosen such that upon failure of one gyro, say $\omega_1$, the magnitude of $E_1$ exceeds the threshold before the magnitude of any of the other $E_i$, for any combination of errors from the other correctly functioning gyros. Of these error combinations the largest error detection threshold can be derived by considering the situation in which the errors in the correctly functioning gyros, $\omega_1$ to $\omega_4$, are $+\delta G$, $-\delta G$, $-\delta G$ and $-\delta G$ respectively. If $\omega_2$ fails such that its output moves in a negative direction from the initial error position ($-\delta G$), the error in the $\omega_2$ output can be expressed as $(-\delta G - Z)$. Substituting these values into equations (4) and (5),

$$ E_1 = \frac{6\delta G}{4} + \frac{Z}{4} $$

$$ E_2 = -\frac{2\delta G}{4} - \frac{3Z}{4}. $$

The magnitude of $E_2$ will exceed that of $E_1$ whenever $+Z$ is more positive than $+2\delta G$, i.e. when the magnitude of $E_2$ is larger than $2\delta G$. Therefore the threshold $T_a$ is chosen to be just greater than $2\delta G$.

A similar argument shows that $T_b$ should also be set just greater than $2\delta G$. In both cases the error detection algorithms will correctly identify any failed gyro assuming that only one failure exists in the system at any one time.

### 3.3. Failure Transients

The 'maximum' pre-detection transient (see section 2.1.4) occurs when a gyro fails such that the error in its output changes from that allowed as a tolerance on a correctly functioning gyro to the maximum value that causes the relevant error detection algorithm to just exceed $2\delta G$.

Consider a failure of $\omega_1$ from an initial error $+\delta G$ to some larger negative value. If the errors in the outputs $\omega_2$, $\omega_3$ and $\omega_4$ are all $-\delta G$, substitution into equation (4) shows that $E_1$ will exceed $-2\delta G$ negatively when $\omega_1$ is less than $-\frac{11}{3}\delta G$. Thus the change in $\omega_1$ before cut out is from $+\delta G$ to $-\frac{11}{3}\delta G$, i.e. $\frac{14}{3}\delta G$. Substituting into the output expression for $p$ (equation (1)) gives the 'maximum' pre-detection transient as $\frac{7}{6}\delta G$.

The largest value attainable by $E_1$ when all gyros are functioning correctly is $\frac{6}{4}\delta G$ (for errors $+\delta G$, $-\delta G$, $-\delta G$, $-\delta G$ in $\omega_1$, $\omega_2$, $\omega_3$, $\omega_4$ respectively). Thus even if $\omega_1$ now fails such that its output moves in a positive direction a change in the error in $\omega_1$ of $\frac{2}{3}\delta G$ is necessary before $E_1$ exceeds $2\delta G$ thus cutting out $\omega_1$. Hence the 'minimum' pre-detection failure transient is $\frac{1}{6}\delta G$.

Thus the pre-detection transient for the first failure will be between $\delta G/6$ and $7\delta G/6$.

Following the decision to disconnect $\omega_1$ the change in output is given by $p - {}_1p$. Now, from equations (1) and (2)

$$ p - {}_1p = \tfrac{1}{4}(\omega_1 + \omega_2 + \omega_3 + \omega_4) - \tfrac{1}{3}(\omega_2 + \omega_3 + \omega_4) $$

$$ = \frac{1}{3}\left(\frac{3\omega_1 - \omega_2 - \omega_3 - \omega_4}{4}\right) $$

$$ = \tfrac{1}{3}E_1 \qquad \text{from equation (4).} $$

But at disconnection $E_1 = T_a = \pm 2\delta G$ hence the magnitude of the switch-over transient will always be $\frac{2}{3}\delta G$.

To obtain the second failure transient, assume that $\omega_2$ fails from an initial error of $+\delta G$, $\omega_1$ already having failed. If the errors in the outputs $\omega_3$ and $\omega_4$ are both equal to $-\delta G$, substitution in equation (8) shows that ${}_1E_2$ will exceed $-2\delta G$ negatively when the error in $\omega_2$ is less than $-4\delta G$. Thus the change in $\omega_2$ before cut out is from $+\delta G$ to $-4\delta G$, i.e. $5\delta G$. Substituting into the output expression for ${}_1p$ (equation (2)) gives the 'maximum' pre-detection transient for a second failure as $\frac{5}{3}\delta G$.

The largest value attainable by ${}_1E_2$ when the remaining three gyros are functioning correctly is $\frac{4}{3}\delta G$ (for errors $+\delta G$, $-\delta G$, $-\delta G$ in $\omega_2$, $\omega_3$, $\omega_4$ respectively). Thus even if $\omega_2$ fails such that its output moves in a positive direction a change in the error in $\omega_2$ of $\delta G$ is necessary before ${}_1E_2$ exceeds $2\delta G$ thus cutting out $\omega_2$. Hence the 'minimum' pre-detection transient for a second failure is $\frac{1}{3}\delta G$.

Thus the pre-detection transient upon second gyro failure will lie between $\frac{5}{3}\delta G$ and $\frac{1}{3}\delta G$.

Following the decision to disconnect $\omega_2$ the change in output is given by ${}_1p - {}_{12}p$. Now, from equations (2) and (3),

$$
\begin{aligned}
{}_1p - {}_{12}p &= \tfrac{1}{3}(\omega_2+\omega_3+\omega_4) - \tfrac{1}{2}(\omega_3+\omega_4) \\
&= \frac{1}{2}\left(\frac{2\omega_2-\omega_3-\omega_4}{3}\right) \\
&= \tfrac{1}{2}({}_1E_2) \qquad \text{from equation (8).}
\end{aligned}
$$

But at disconnection ${}_1E_2 = T_b = \pm 2\delta G_g$ hence the magnitude of the switch-over transient will always be $\delta G$.

The transients are summarised in Table 1.

### 3.4. Failure Probability

In this Twelve Gyro Orthogonal Arrangement the three sets of four gyros, one set in each axis, can be assumed to be independent. Thus, since the loss of three gyros in any one axis will cause loss of control, the probability of three out of four gyros failing is given by $(4.2.3)\hat{p}^3/(1.2.3) = 4\hat{p}^3$, where $\hat{p}$ is the probability of any one gyro failing. Therefore the probability of loss of control in at least one of the three axes is $12\hat{p}^3$.

### 3.5. Interface with Power Supplies and System Computers

Fig. 3 shows the interface between the four sets of gyros and a quadruplex power supply and computing configuration. Each set of three gyros (one pitch, one roll and one yaw) is associated with a computer and a common power supply so that loss of one computer or one power supply implies loss of one set of gyro information. This is a straightforward implementation and follows well known system design principles.

### 3.6. Battle Damage

As discussed in Section 2.4, the problem of battle damage survival leads to considering dispersion of the sensors around the aircraft. Since the four sets of gyros (one pitch, one roll and one yaw) are independent they could be positioned at four different locations such that a single shell hit would only destroy one set. In this case only one gyro in each axis would appear to have failed and hence the error detection algorithms would correctly identify the failure. Positioning of the gyros in only two or three different locations would require the application of more complex algorithms since two gyros in each set could be destroyed simultaneously.

## 4. The Eight Gyro Pyramid

The cross transfer of sensor data between lanes for consolidation purposes allows systems to be considered in which the two failure survival capability can be achieved with less than twelve sensors. As mentioned earlier, an analysis of a six gyro scheme has shown that the failure transients can be several times larger than those of the Twelve Gyro Orthogonal Arrangement. This is considered to be unacceptable and led to the development of the following Eight Gyro Arrangement.

### 4.1. Pyramid Measurement Axes

Consider four measurement axes aligned along the edges of a pyramid (Fig. 5), the pyramid having its apex at the origin of the aircraft axes. The base of the pyramid is normal to one axis (say the $x$ axis) and

adjacent edges of the base are parallel to the other two axes ($y$ and $z$ axes). If four pairs of gyros are mounted such that each pair has its measurement axis along one of the edges of the pyramid the angle subtended by any pair axis with the $x$ aircraft axis will be of equal magnitude for all pairs. Similarly the angles subtended with the other axes will be of equal magnitude for all the gyro pairs although the actual angles between the axes may be different. Let these angles be of modulus $\alpha_p$, $\alpha_q$ and $\alpha_r$ relative to the $x$, $y$ and $z$ axes respectively, and let eight gyros with outputs $\omega_1, \omega_2, \omega_3, \ldots, \omega_8$ be mounted as in Fig. 5, such that ($\omega_1$ and $\omega_5$), ($\omega_2$ and $\omega_6$), ($\omega_3$ and $\omega_7$) and ($\omega_4$ and $\omega_8$) are parallel pairs.

Then for rates $p$(roll), $q$(pitch) and $r$(yaw) about the $x$, $y$ and $z$ axes respectively, and with the cosines of $\alpha_p$, $\alpha_q$ and $\alpha_r$ equal to $C_p$, $C_q$ and $C_r$

$$\left.\begin{aligned}
\omega_1 = \omega_5 &= pC_p + qC_q + rC_r \\
\omega_2 = \omega_6 &= pC_p - qC_q + rC_r \\
\omega_3 = \omega_7 &= pC_p + qC_q - rC_r \\
\omega_4 = \omega_8 &= pC_p - qC_q - rC_r
\end{aligned}\right\} \tag{11}$$

Solving these equations for $p$, $q$ and $r$ (by addition and subtraction in pairs) gives eight expressions for each.

The roll rate $p$ is given by

$$\begin{aligned}
&\frac{1}{2C_p}(\omega_1+\omega_4), \quad \frac{1}{2C_p}(\omega_5+\omega_4), \quad \frac{1}{2C_p}(\omega_1+\omega_8), \quad \frac{1}{2C_p}(\omega_5+\omega_8) \\
&\frac{1}{2C_p}(\omega_2+\omega_3), \quad \frac{1}{2C_p}(\omega_6+\omega_3), \quad \frac{1}{2C_p}(\omega_2+\omega_7) \quad \text{and} \quad \frac{1}{2C_p}(\omega_6+\omega_7).
\end{aligned} \tag{12}$$

The pitch rate $q$ is given by

$$\begin{aligned}
&\frac{1}{2C_q}(\omega_1-\omega_2), \quad \frac{1}{2C_q}(\omega_1-\omega_6), \quad \frac{1}{2C_q}(\omega_5-\omega_2), \quad \frac{1}{2C_q}(\omega_5-\omega_6) \\
&\frac{1}{2C_q}(\omega_3-\omega_4), \quad \frac{1}{2C_q}(\omega_3-\omega_8), \quad \frac{1}{2C_q}(\omega_7-\omega_4) \quad \text{and} \quad \frac{1}{2C_q}(\omega_7-\omega_8).
\end{aligned} \tag{13}$$

The yaw rate $r$ is given by

$$\begin{aligned}
&\frac{1}{2C_r}(\omega_1-\omega_3), \quad \frac{1}{2C_r}(\omega_1-\omega_7), \quad \frac{1}{2C_r}(\omega_5-\omega_3), \quad \frac{1}{2C_r}(\omega_5-\omega_7) \\
&\frac{1}{2C_r}(\omega_2-\omega_4), \quad \frac{1}{2C_r}(\omega_2-\omega_8), \quad \frac{1}{2C_r}(\omega_6-\omega_4) \quad \text{and} \quad \frac{1}{2C_r}(\omega_6-\omega_8).
\end{aligned} \tag{14}$$

### 4.2. Pyramid Algorithms

Since eight estimates of the aircraft's rate of rotation exist for each axis a significant degree of redundancy of information is available. Many methods exist by which these signals can be combined to form consolidated outputs. Similarly a range of error detection algorithms can be defined. The choice of the particular set of algorithms defined for a system depends not only upon the requirements described in Section 2 but additionally on other items such as ease of comprehension, previous experience, implementation technology, gyro failure characteristics and aircraft response. A complete evaluation of the range of algorithms was not undertaken although several alternatives have been considered during this study. Three sets have been chosen for presentation in this paper, each demonstrating particular attributes of the pyramid organisation.

Set A was chosen to permit the use of the algorithms previously described in Section 3 for the Twelve Gyro Orthogonal Arrangement. No new algorithm development is involved, and, in fact, any algorithms applicable to the Twelve Gyro Orthogonal Arrangement can equally well be applied in this manner to the Eight Gyro Pyramid.

In Set B two forms of error detection algorithms are used, the first to detect that a failure has occurred and the second to determine which gyro has failed. By this means the failure transients can be reduced in comparison with those of the Set A algorithm.

The Set C algorithms are a modified version of the Set B, incorporating a self-detecting battle damage capability.

The next two sections of this Report describe the analysis of these alternatives. As a comparative guide, the failure transients for the three algorithm sets are shown compared with those of the Twelve Gyro Orthogonal Arrangement, in Tables 2 and 3. It can be seen that for all three algorithm sets the increase in the size of the transient over that experienced with the Twelve Gyro Orthogonal Arrangement is always less than 1·75. Hence only a modest increase in the quality of the gyros used would overcome this deficiency. Alternatively, the pyramid arrangement is such that by varying the direction cosines it is possible to reduce this ratio in one axis if larger transients are acceptable in the other axes.

## 5. Pyramid Algorithm Set A

The gyro outputs can be combined in pairs as in equations (12), (13) and (14) to give eight estimates of $2pC_p$, $2qC_q$ and $2rC_r$. Consider only those estimates which are independent as far as the individual control axes are concerned. These are

$$\left.\begin{array}{llll} 2pC_p = \omega_1+\omega_4, & \omega_2+\omega_3, & \omega_5+\omega_8, & \omega_6+\omega_7 \\ 2qC_q = \omega_1-\omega_2, & \omega_3-\omega_4, & \omega_5-\omega_6, & \omega_7-\omega_8 \\ 2rC_r = \omega_1-\omega_3, & \omega_2-\omega_4, & \omega_5-\omega_7, & \omega_6-\omega_8. \end{array}\right\} \quad (15)$$

Each axis now has four independent estimates which can be combined in exactly the same manner as described in Section 3. Whereas in the Twelve Gyro Orthogonal Arrangement each estimate is a single gyro output, with maximum error $\delta G$, in this pyramid set each estimate is formed from two gyro outputs and is scaled by a factor $1/C_p$ for the roll rate output (see Fig. 8). Thus the equivalent maximum allowable error on a pyramid estimate is, for roll rate,

$$\frac{1}{C_p}\left(\frac{\delta G+\delta G}{2}\right)=\frac{\delta G}{C_p}$$

i.e. the effective tolerance on a correctly functioning gyro estimate has been increased by a factor of $1/C_p$. Hence the algorithms of Section 3 can be used giving output and error detection algorithms as listed in Appendix A. It should be noted that a difference set of error detection algorithms will exist for each axis of control.

Using the gyro outputs to form the above 'independent' estimates allows the pyramid system to be used with any algorithm set applicable to the Twelve Orthogonal Arrangement. In this form no new algorithm development is necessary and hence the Eight Gyro Pyramid could be designed as a 'stand alone' package to interface with any system designed for a Twelve Gyro Orthogonal Arrangement.

### 5.1. Failure Transients

Since the output and error detection algorithms are identical to those used for the Twelve Gyro Orthogonal Arrangement but with the maximum allowable error ($\delta G$) in a valid estimate scaled by $1/C_p$, $1/C_q$ and $1/C_r$, the failure transients are the same as those developed in Section 3 but with $\delta G$ replaced by $\delta G/C_p$, $\delta G/C_q$ and $\delta C/C_r$ in the roll, pitch and yaw axes respectively. The $C_p$, $C_q$ and $C_r$ are cosines and therefore are less than unity hence the failure transients for the Set A algorithms are larger than those for the Twelve Gyro Orthogonal Arrangement. It should be noted that a transient will occur in all three axes whenever a gyro fails.

*5.1.1. Selection of Direction Cosines.* The direction cosines are related by the expression $C_p^2+C_q^2+C_r^2=1$. Hence two can be chosen to minimise the disconnect transient in pitch and roll (say) at the expense of that in yaw, the larger the direction cosine the smaller the disconnect transient.

A discussion of the relative merits of reducing the transients in one axis rather than another is beyond the scope of this paper. For simplicity $C_p$, $C_q$ and $C_r$ have been assumed to be equal, giving a value of $1/\sqrt{3}$. Hence the failure transients are increased by 1·73 compared with those of the Twelve Gyro Orthogonal

Arrangement, and are shown in Table 2 and also in Table 3 as a ratio of the failure transients of the Twelve Gyro Orthogonal Arrangement.

### 5.2. Failure Probability

The interdependence of the estimates used for the pitch, roll and yaw axes increases the probability of loss of control in comparison with that of the Twelve Gyro Orthogonal Arrangement. As before, let $\hat{p}$ be the probability of failure of any one gyro.

Consideration of the four independent estimates used in each of the three axes (see equation (15)) shows that at least three gyros must fail before control is lost in any axis. It can also be seen that not all combinations of three failed gyros lead to loss of control. In particular, loss of three gyros in Group I containing ($\omega_1$, $\omega_2$, $\omega_3$ and $\omega_4$) or loss of three gyros in Group II containing ($\omega_5$, $\omega_6$, $\omega_7$ and $\omega_8$) does not result in loss of control since two estimates of $p$, $q$ and $r$ remain. Loss of control in at least one axis occurs with three gyro failures only when two failures are in Group I or Group II and the third failure is in the other group.

The probability of two gyro failures in a group of four gyros is

$$\frac{4.3}{2}\hat{p}^2 = 6\hat{p}^2.$$

Thus the probability of two failures in either Group I or Group II is $12\hat{p}^2$. This latter probability is multiplied by $4\hat{p}$, the probability of one failure in a group of four gyros, to give the probability of loss of control as $48\hat{p}^3$. This is four times higher than that for the Twelve Gyro Orthogonal Arrangement.

### 5.3. Interface with Power Supplies and System Computers

At first sight, a quadruplex power supply arrangement would appear to interface satisfactorily if each supply is fed to one pair of gyros. However, failure of two supplies could deprive the system of four gyro outputs, which for the combinations described in Section 5.2 will lead to loss of control. It is necessary therefore to use a more complex power supply arrangement, namely, that power supply consolidation must be used to ensure that loss of a supply does not cause loss of more than one gyro output.

Similarly the simple computer interface, shown in Fig. 9a, in which two gyros are fed directly to each computer and the other gyro outputs are received via the cross feeds will not always survive the loss of two computers since, as above, four gyro outputs will be lost. An acceptable arrangement is shown in Fig. 9b whereby each gyro feeds information directly to two computing lanes so that the loss of two computers can only deprive the remaining system of two gyro outputs. In this situation early recognition of the loss of the second computer, due to either malfunction or loss of the power supply, is necessary if the error detection algorithms are not to malfunction as a result of losing two gyro outputs at the same time.

### 5.4. Battle Damage

The Set A error detection algorithms can only isolate failure of one gyro at a time, hence any installation in which the gyros are grouped together must use a different detection system to ascertain when a shell hit has destroyed a particular group. The alternative is to mount the eight gyros in eight separate locations, a more difficult requirement than that of the Twelve Gyro Orthogonal Arrangement.

## 6. Pyramid Algorithm Set B

The set A algorithms were derived from those used as a base line for the Twelve Gyro Orthogonal Arrangement. Only four of the eight estimates available in each axis were used; the Set B algorithms discussed in this section use all eight estimates to reduce the magnitude of the 'maximum' failure transients. As mentioned earlier, the Set B algorithms are one of a number of options and may well not be the 'optimum'; an additional Set C is also described to indicate how a self-detecting battle damage capability can be obtained.

In order to simplify the text only the roll axis algorithms are derived. Identical algorithms exist for the other axes and are shown in Appendix B.

### 6.1. Set B Consolidation Algorithms

The eight estimates of roll rate ($p$) derived from the gyro outputs in Section 4.1 were

$$\frac{1}{2C_p}(\omega_1+\omega_4),\quad \frac{1}{2C_p}(\omega_5+\omega_4),\quad \frac{1}{2C_p}(\omega_1+\omega_8),\quad \frac{1}{2C_p}(\omega_5+\omega_8),$$

$$\frac{1}{2C_p}(\omega_2+\omega_3),\quad \frac{1}{2C_p}(\omega_6+\omega_3),\quad \frac{1}{2C_p}(\omega_2+\omega_7)\quad \text{and}\quad \frac{1}{2C_p}(\omega_6+\omega_7). \tag{16}$$

When all eight gyros are functioning correctly the output $p$ is chosen as the average of these eight estimates, hence

$$p=\frac{1}{16C_p}(2\omega_1+2\omega_2+2\omega_3+2\omega_4+2\omega_5+2\omega_6+2\omega_7+2\omega_8). \tag{17}$$

As can be seen from (16) the loss of any one gyro (say $\omega_1$) invalidates two estimates. Thus the output with seven working gyros is chosen to be the average of the remaining six estimates, i.e.

$$_1p=\frac{1}{12C_p}(2\omega_2+2\omega_3+\omega_4+2\omega_5+2\omega_6+2\omega_7+\omega_8), \tag{18}$$

Similar output expressions exist for all first failures.

Three groups of second failure exist. A parallel pair failure, e.g. $\omega_1$ and $\omega_5$, leaves four valid estimates. Hence the output is chosen as

$$_{15}p=\frac{1}{4C_p}(\omega_2+\omega_3+\omega_6+\omega_7).$$

Inspection of the estimates (16) shows that after a failure of $\omega_1$ (say), two classes of non-parallel second failure exist, those whose failure would reduce the number of valid estimates to four and those that would leave five valid estimates. Consideration of the valid estimates remaining in all three axes following any second non-parallel failure shows that four estimates will remain valid in two axes whilst there will always be five in the third axis.

The output expression for the roll axis for each of these two classes of failure is represented by considering for the first class an $\omega_1$ and $\omega_2$ failure combination giving four estimates. Hence the output is

$$_{12}p=\frac{1}{8C_p}(\omega_3+\omega_4+2\omega_5+2\omega_6+\omega_7+\omega_8)$$

and for the second class an $\omega_1$ and $\omega_4$ failure combination giving five valid estimates so

$$_{14}p=\frac{1}{10C_p}(2\omega_2+2\omega_3+\omega_5+2\omega_6+2\omega_7+\omega_8).$$

Similar output expressions exist for all the other gyro failure combinations.

The output expressions for first and second failures in all three axes are given in Appendix B.

Certain combinations of three gyro failures can be survived whilst others are catastrophic even though at least two valid estimates always remain. The difficulty is in correctly identifying the third failure. The error detection algorithms described in the next section will correctly identify third and fourth failures, if and only if no two failed gyros are a parallel pair.

### 6.2. Set B Error Detection Algorithms

A general error detection algorithm is derived by differencing the eight estimates of $2pC_p$ (from equation (11)) as follows:

$$E=(\omega_1+\omega_4)-(\omega_2+\omega_3)+(\omega_5+\omega_8)-(\omega_6+\omega_7),$$

i.e.

$$E=\omega_1-\omega_2-\omega_3+\omega_4+\omega_5-\omega_6-\omega_7+\omega_8.$$

Since the gyros are mounted as four sets of parallel pairs this general error algorithm can be particularised by substituting the relevant outputs (e.g. $\omega_1$ for $\omega_5$, $\omega_2$ for $\omega_6$ etc.) to give eight error detection algorithms:

$$E_1 = 2\omega_1 - \omega_2 - \omega_3 + \omega_4 - \omega_6 - \omega_7 + \omega_8 \tag{19}$$

$$E_2 = \omega_1 - 2\omega_2 - \omega_3 + \omega_4 + \omega_5 - \omega_7 + \omega_8 \tag{20}$$

$$E_3 = \omega_1 - \omega_2 - 2\omega_3 + \omega_4 + \omega_5 - \omega_6 + \omega_8 \tag{21}$$

$$E_4 = \omega_1 - \omega_2 - \omega_3 + 2\omega_4 + \omega_5 - \omega_6 - \omega_7 \tag{22}$$

$$E_5 = -\omega_2 - \omega_3 + \omega_4 + 2\omega_5 - \omega_6 - \omega_7 + \omega_8 \tag{23}$$

$$E_6 = \omega_1 - \omega_3 + \omega_4 + \omega_5 - 2\omega_6 - \omega_7 + \omega_8 \tag{24}$$

$$E_7 = \omega_1 - \omega_2 + \omega_4 + \omega_5 - \omega_6 - 2\omega_7 + \omega_8 \tag{25}$$

$$E_8 = \omega_1 - \omega_2 - \omega_3 + \omega_5 - \omega_6 - \omega_7 + 2\omega_8. \tag{26}$$

A second set of error algorithms are used, formed by taking the difference between parallel gyros.

$$E_9 = \omega_1 - \omega_5 \tag{27}$$

$$E_{10} = \omega_2 - \omega_6 \tag{28}$$

$$E_{11} = \omega_3 - \omega_7 \tag{29}$$

$$E_{12} = \omega_4 - \omega_8. \tag{30}$$

A failure detection threshold $S_a$ is associated with the magnitude of the $E_9$ to $E_{12}$. Whenever this is exceeded the relevant $E$ will indicate that one of a particular pair of gyros is suspect, e.g. if the magnitude of $E_9$ exceeds the threshold $S_a$ then either $\omega_1$ or $\omega_5$ has failed. Following such a failure indication the $E_1$ to $E_8$ are used to isolate the failure. Since it is known which pair of gyros are suspect only two of the set $E_1$ to $E_8$ need be considered. In the example only the magnitudes of $E_1$ and $E_5$ need be inspected to ascertain which has exceeded the threshold $S_b$. Since comparison of the expressions for $E_1$ and $E_5$ shows that they both contain identical sums of the non-suspect gyros and since each is dependent only upon one of the suspect gyros the failed gyro is always correctly identified. As with all voters it has been assumed that only one gyro fails at a time.

Whenever a gyro has been identified as having failed its output is replaced in all the error detection algorithms above by the output of the parallel gyro. Hence following an $\omega_1$ failure, replacing $\omega_1$ by $\omega_5$ gives

$${}_1E_2 = -2\omega_2 - \omega_3 + \omega_4 + 2\omega_5 - \omega_7 + \omega_8$$

$${}_1E_3 = -\omega_2 - 2\omega_3 + \omega_4 + 2\omega_5 - \omega_6 + \omega_8$$

$${}_1E_4 = -\omega_2 - \omega_3 + 2\omega_4 + 2\omega_5 - \omega_6 - \omega_7$$

$${}_1E_5 = E_5 = -\omega_2 - \omega_3 + \omega_4 + 2\omega_5 - \omega_6 - \omega_7 + \omega_8$$

$${}_1E_6 = -\omega_3 + \omega_4 + 2\omega_5 - 2\omega_6 - \omega_7 + \omega_8$$

$${}_1E_7 = -\omega_2 + \omega_4 + 2\omega_5 - \omega_6 - 2\omega_7 + \omega_8$$

$${}_1E_8 = -\omega_2 - \omega_3 + 2\omega_5 - \omega_6 - \omega_7 + 2\omega_8$$

$${}_1E_9 = \text{ZERO}$$

$${}_1E_{10} = E_{10} = \omega_2 - \omega_6$$

$${}_1E_{11} = E_{11} = \omega_3 - \omega_7$$

$${}_1E_{12} = E_{12} = \omega_4 - \omega_8.$$

Consider the situation when a second gyro fails following a failure of $\omega_1$, say. As only one failure is assumed to occur at a time, whenever the magnitude of one of the ${}_1E_{10}$, ${}_1E_{11}$ or ${}_1E_{12}$ exceeds the failure detection threshold $S_a$ the relevant pair of the ${}_1E_2$ to ${}_1E_8$ are inspected. The same argument as used for the first failure case still applies and hence when the magnitude of one of this set of algorithms exceeds the $S_b$ threshold the failure has been correctly identified.

A slightly different technique must be used for $\omega_5$ since ${}_1E_9$ is no longer a valid error detector. If the magnitudes of ${}_1E_{10}$, ${}_1E_{11}$ and ${}_1E_{12}$ do not exceed the threshold $S_a$ then the six gyros $\omega_2$, $\omega_3$, $\omega_4$, $\omega_6$, $\omega_7$ and $\omega_8$ are functioning correctly. Error detector ${}_1E_5$ contains these six gyros plus $\omega_5$ and so can be used as a direct test for $\omega_5$. The only modification necessary is to use a slightly larger error detection threshold $S_c$ for ${}_1E_5$. This is derived with the other thresholds in Section 6.2.1.

In general the system enables two gyro failures to be survived. However the technique of using one of the $E_9$ to $E_{12}$ to indicate a failure and then using the relevant $E_1$ to $E_8$ to isolate the failure to a particular gyro will correctly identify third and fourth failures if and only if no two failed gyros are parallel. If two non-parallel gyros have failed then their outputs can be replaced in the error detection algorithms by their parallel equivalents. This gives two identical error detection algorithms for the two gyros that are parallel to one or other of the failed gyros; hence a failure of either of these gyros cannot be isolated.

These error detection algorithms are absolute indicators of the failure of particular gyros and not of an estimate failure as in the Set A algorithms described earlier. Hence these algorithms are equally applicable to all axes.

*6.2.1. Error Detection Thresholds.* The maximum difference between the outputs of any two correctly functioning parallel gyros is $2\delta G$. Thus the threshold $S_a$ for the $E_9$, $E_{10}$, $E_{11}$ and $E_{12}$ is set at $2\delta G$. Exceeding this threshold indicates failure of one of a particular pair of gyros.

The maximum value of $E_1$ to $E_8$ when all eight gyros are functioning correctly is $8\delta G$. Thus the threshold $S_b$ for the $E_1$ to $E_8$ is set at $8\delta G$. Exceeding this threshold indicates failure of one of seven gyros but does not, by itself, isolate the failed gyro. However the combination of one of the magnitudes of the $E_9$ to $E_{12}$ exceeding the threshold $2\delta G$ and so indicating failure of one of a particular pair of gyros, followed by the magnitude of the error detector for one of this pair exceeding $8\delta G$, uniquely identifies the failed gyro. It should be noted that for particular combinations of the errors in the seven correctly functioning gyros a situation can arise in which the relevant $E_1$ to $E_8$ will have a value of up to $12\delta G$ before one of the $E_9$ to $E_{12}$ indicates a failure, e.g. let $\omega_1$ fail positively from an initial error $+\delta G$ when the other gyros, $\omega_2$ to $\omega_8$, have errors $-\delta G$, $-\delta G$, $+\delta G$, $+\delta G$, $-\delta G$, $-\delta G$, $+\delta G$ respectively. $E_9$ will indicate a failure of $\omega_1$ or $\omega_5$ when the error in $\omega_1$ is $+3\delta G$, at which time $E_1$ will have a value $12\delta G$ and $E_5$ will have a value $8\delta G$. Hence it is essential to identify a failure only when the magnitude of one of the $E_9$ to $E_{12}$ exceeds $2\delta G$.

Following failure and isolation of gyro $\omega_1$, only one error detection equation remains for gyro $\omega_5$:

$$ {}_1E_5 = -\omega_2 - \omega_3 + \omega_4 + 2\omega_5 - \omega_6 - \omega_7 + \omega_8. $$

In contrast to failures of the other gyros ($\omega_2$, $\omega_3$, $\omega_4$, $\omega_6$, $\omega_7$, $\omega_8$) which still have two valid sets of equations and hence can detect and isolate failures as described above, failure of $\omega_5$ must be detected and isolated by this one equation. In particular the threshold $S_c$ set for ${}_1E_5$ must ensure that failures of gyros other than $\omega_5$ do not cause incorrect identification of the failed gyro. Suppose, for example, $\omega_4$ fails in a positive direction from a condition where the errors in the outputs of $\omega_2$ to $\omega_8$ are initially $-\delta G$, $-\delta G$, $+\delta G$, $+\delta G$, $-\delta G$, $-\delta G$, $+\delta G$ respectively. The error in $\omega_4$ will be $3\delta G$ before ${}_1E_{12}$ exceeds $2\delta G$. Substituting these values into ${}_1E_5$ shows that it can have a value of $10\delta G$. Hence the threshold $S_c$ is set at $10\delta G$ to ensure that failures of other gyros are correctly identified by the error detection algorithms.

### 6.3. Failure Transients

The 'maximum' failure transients for both first and second failures are derived in Appendix C and are shown in Tables 2 and 3. It can be seen that the Set A and Set B switch-over transients are the same but that the Set B have lower pre-detection transients. Also, as before, a transient will occur in all three axes whenever a gyro fails.

As in the case of the pyramid Set A algorithms the failure transients in any axis are inversely proportional to the direction cosine of the angle between the edges of the pyramid and the aircraft axis. The transients in any axis can be reduced at the expense of those in another axis as described in Section 5.1.1.

Also derived in Appendix C and shown in Tables 2 and 3 are the 'minimum' failure transients. In the case of the pyramid Set B algorithms a zero pre-detection may be experienced and the switch-over transient may be smaller than in the Twelve Gyro Orthogonal Arrangement.

### 6.4. Failure Probability

Loss of control for the Set B algorithms occurs when any parallel pair of gyros plus any one other gyro fail. Let the probability of any one gyro failing be $\hat{p}$.

The probability of failure of one pair of the four parallel pairs of gyros is $4\hat{p}^2$. The probability of failure of one of the other six gyros is $6\hat{p}$. Hence the probability of loss of control due to three gyro failures is $24\hat{p}^3$. This is twice as high as that for the Twelve Gyro Orthogonal Arrangement and half that of the Set A algorithms.

### 6.5 Interface with Power Supplies and System Computers

The same approach as with the Set A algorithms described in Section 5.3 is valid, namely that the four power supplies must be consolidated to ensure that loss of a supply does not cause loss of more than one gyro output. Similarly the computer interface shown in Fig. 9b is again valid and the same criticism is relevant, namely that early recognition of the loss of two computers, due to malfunction or to loss of two power supplies, is necessary if the error detection algorithms are not to malfunction as a result of losing two gyro outputs at the same time.

### 6.6. Battle Damage (Set C Error Detection Algorithms)

The Set A error detection algorithms were not capable of indicating the loss of a set of gyros due to battle damage unless eight separate gyro locations were available. This is also true of the Set B algorithms. A slight modification to the Set B error detection technique overcomes this deficiency and makes the problem with the pyramid solution similar to that of the Twelve Gyro Orthogonal Arrangement, namely, if four separate mounting locations are available then a shell hit upon a gyro package can be detected.

For the Set C algorithms the gyros are assumed to be mounted in the pairs shown in Fig. 9b, namely as four sets containing respectively ($\omega_1$ and $\omega_2$), ($\omega_3$ and $\omega_4$), ($\omega_5$ and $\omega_6$) and ($\omega_7$ and $\omega_8$). The error detection equations of Set B (Section 6.2) are modified such that in error detectors $E_1$ and $E_2$, $\omega_5$ and $\omega_6$ are replaced by $\omega_1$ and $\omega_2$ (their parallel equivalents), and similarly with the other error detectors $E_3$ to $E_8$. Equations (19) to (26) become:

$$
\begin{aligned}
E_1 = E_2 &= 2\omega_1 - 2\omega_2 - \omega_3 + \omega_4 - \omega_7 + \omega_8 \\
E_3 = E_4 &= \omega_1 - \omega_2 - 2\omega_3 + 2\omega_4 + \omega_5 - \omega_6 \\
E_5 = E_6 &= -\omega_3 + \omega_4 + 2\omega_5 - 2\omega_6 - \omega_7 + \omega_8 \\
E_7 = E_8 &= \omega_1 - \omega_2 + \omega_5 - \omega_6 - 2\omega_7 + 2\omega_8.
\end{aligned}
$$

The $E_9$ to $E_{12}$ are still used with the same threshold $S_a$ to indicate a failure of one of a parallel pair of gyros and the relevant $E_1$ to $E_8$ are inspected to isolate the failure using the $S_b$ threshold. Following a failure the relevant gyro output is replaced by its parallel equivalent and the Set B procedure followed except that a new threshold $S_d$ must be used for the algorithm detecting a failure of the gyro parallel to the failed gyro. If the analysis of Section 6.2.1 is repeated using the Set C algorithms it will be seen that $S_d$ must be set equal to $12\delta G$. Using this level and repeating the failure transient analysis of Appendix C gives the Set C failure transients shown in Tables 2 and 3.

Consider now the shell hit survival requirement namely that assuming no other failures a single shell hit must be survived. Assume that gyros $\omega_1$ and $\omega_2$ are destroyed. It is probable that the magnitudes of $E_9$ and $E_{10}$ will simultaneously exceed the threshold $S_a$. If this occurs either the pair ($\omega_1$ and $\omega_2$) or the pair ($\omega_5$ and $\omega_8$) should be assumed to have failed. The uncertainty is resolved by considering which of the error detectors $E_1$ (equal to $E_2$) or $E_5$ (equal to $E_6$) has a magnitude greater than the threshold $S_b$.

The disadvantage of the Set C algorithms described above, namely that the failure transients are larger than those of the Set B, can be overcome by using both sets of algorithms within the system, only referring to the Set C when a dual failure apparently occurs.

## 7. Discussion

As has been seen the reduction from twelve to eight in the number of gyros used to provide a two failure survival three-axis pyramid sensor set inevitably means that certain features of the system are degraded. In particular the maximum failure transients may be slightly larger (an increase by a factor less than 1·73) and the probability of loss of control is increased by a factor less than 4 for the algorithm sets described. These factors are not considered to be large even for the Set A algorithms where the solution readily interfaces with conventional multiplex designs and utilises identical algorithms to those of the Twelve Gyro Orthogonal Arrangement. This has been achieved with a solution which could be built as a stand-alone package if gyro signal isolation is ensured.

A small improvement in the quality of the rate sensor used would overcome the above deficiency but will still leave a situation in which the error detection algorithms are different in each control axis and also, following a gyro failure, some valid information is not being utilised. Further development has shown that by utilising different algorithms the failure transient characteristics can be beneficially modified and in the case of the Set B and Set C algorithms, the probability of loss of control halved in comparison with that for Set A. The algorithms that have been presented are intended as examples only; further work may reveal that other sets of algorithms could improve the situation still further.

A feature of multiplex flight control systems not discussed earlier is that of the pre-flight checkout. This is considered essential and it has been proposed that it can be achieved in the Twelve Gyro Orthogonal Arrangement by pairs comparisons. The same technique can be applied to the pyramid system since every gyro has a parallel partner.

An area of study not pursued during this investigation is associated with the relative importance of failure transients in each of the aircraft's axes which can be modified by the choice of the direction cosines of the pyramid. Some additional work is required to establish the relevant tradeoffs. An investigation is also required into the feasibility of using widely spaced sensor mounting locations to provide shell hit survival.

During the development of the eight gyro system described, other pyramid configurations using four or twelve gyros have been considered briefly. A three-axis 'fail safe' (i.e. duplex) system can be produced by using four gyros mounted one along each edge of the pyramid. This will provide two output estimates in each axis and is hence fail safe using only four gyros rather than the conventional six.

Another promising alternative is that in which twelve gyros are used, sets of three parallel gyros being mounted along each of the edges of the pyramid. This system offers a four gyro failure survival capability and is thus better than the conventional twelve gyro orthogonal approach. A detailed failure transient investigation has not been performed but it is throught that algorithms could be developed in which the first and second failure transients are reduced from those of the Twelve Gyro Orthogonal Arrangement thus having a smaller effect upon the aircraft or alternatively allowing poorer quality gyros to be used.

An additional item of discussion arising during this work has been that of the philosophy to be employed when only two valid estimates remain in an axis of control. Systems to date have proposed averaging these but the failure probability in this case (as with all duplex systems) is twice that achieved if one estimate is ignored.

## 8. Conclusions

An Eight Gyro Pyramid Sensor Set has been described which suffers only a small degradation in performance compared with the conventional Twelve Gyro Orthogonal Arrangement proposed for two failure survival three-axis flight control systems. The new system can be developed either as a stand-alone package to interface with existing consolidation designs or to provide a smaller disconnection transient and lower probability of loss of control using new consolidation algorithms. The reduction in the number of sensors reduces the first time cost and also the probability of a defect occurring and therefore reduces maintenance cost and effort. In addition each gyro experiences an identical input range and so the same type of gyro can be used in all sensing positions.

The pyramid arrangement shows considerable promise and it is recommended that an engineering assessment be made. Additional system benefits can be achieved but further information is required in the areas of sensor location within an airframe to give battle damage protection and in the relative effects of failure transients in the individual aircraft axes.

## LIST OF SYMBOLS

| | |
|---|---|
| $\alpha_p, \alpha_q, \alpha_r$ | Modulus of the angle between an edge of the pyramid and the $x$, $y$ and $z$ axes respectively |
| $C_p, C_q, C_r$ | Cosines of $\alpha_p$, $\alpha_q$ and $\alpha_r$ respectively |
| $E$ | General error detection algorithm |
| $E_i\ i = 1, \ldots 8$ | $i$th gyro error detector |
| $E_i\ i = 9, \ldots 12$ | Parallel pair error detectors |
| ${}_jE_i \begin{matrix} i = 1, \ldots 8 \\ j = 1, \ldots 8 \end{matrix}$ | $i$th gyro error detector, $j$th gyro disconnected |
| $\hat{p}$ | Probability of failure of a gyro |
| $p, q, r$ | Consolidated roll, pitch and yaw outputs |
| ${}_jp, {}_jq, {}_jr$ | Consolidated roll, pitch and yaw outputs but with $j$th gyro disconnected |
| ${}_{jk}p, {}_{jk}q, {}_{jk}r$ | Consolidated roll, pitch and yaw outputs but with $j$th then $k$th gyros disconnected |
| $S_a, S_b, S_c, S_d$ | Pyramid error detection thresholds |
| $T_a, T_b$ | Twelve gyro orthogonal arrangement error detection thresholds |
| $\omega_i$ | The output of the $i$th gyro |
| $z$ | A gyro error level |
| $\delta G$ | The allowable error tolerance on a correctly functioning gyro |

## REFERENCES


| *No.* | *Author(s)* | *Title, etc.* |
|---|---|---|
| 1 | D. Kimberley ..... | Some guidelines and constraints for integrated flight control system studies.<br>Unpublished MOD(PE) material. |
| 2 | P. J. Shipp ..... | Experimental electronic circuits for an integrated manoeuvre demand flight control system.<br>RAE Technical Report 70128 (1970). |
| 3 | D. Kimberley and P. W. J. Fulham .. | Flight control development in the UK.<br>'Advances in Control Systems', AGARD CP137 (1974). |
| 4 | C. R. Abrams and W. D. Weinstein . | The ASSET (Advanced Skewed Sensory Electronic Triad) program.<br>'Impact of Active Control Technology on Airplane Design', AGARD CP157 (1975). |

## APPENDIX A

### Eight Gyro Pyramid Algorithm Set A

### A.1. No Failures

Outputs:

$$p = \frac{1}{8C_p}(\omega_1+\omega_2+\omega_3+\omega_4+\omega_5+\omega_6+\omega_7+\omega_8)$$

$$q = \frac{1}{8C_q}(\omega_1-\omega_2+\omega_3-\omega_4+\omega_5-\omega_6+\omega_7-\omega_8)$$

$$r = \frac{1}{8C_r}(\omega_1+\omega_2-\omega_3-\omega_4+\omega_5+\omega_6-\omega_7-\omega_8).$$

Error detectors:

Roll axis $E_1 = E_4 = \frac{1}{8C_p}(3\omega_1+3\omega_4-\omega_2-\omega_3-\omega_5-\omega_6-\omega_7-\omega_8)$

$E_2 = E_3 = \ldots$ etc.

Pitch axis $E_1 = E_2 = \frac{1}{8C_q}(3\omega_1-3\omega_2-\omega_3-\omega_4-\omega_5+\omega_6-\omega_7+\omega_8)\ldots$ etc.

Yaw axis $E_1 = E_3 = \frac{1}{8C_r}(3\omega_1-3\omega_3-\omega_2+\omega_4-\omega_5-\omega_6+\omega_7+\omega_8)\ldots$ etc.

In all above cases the error detection threshold is $2\delta G/C_p$, $2\delta G/C_q$ and $2\delta G/C_r$ for roll, pitch and yaw respectively.

NOTE: The error detection algorithms are different for each axis of control.

### A.2. After First Failure (say $\omega_1$)

Outputs:

$${}_1p = \frac{1}{6C_p}(\omega_2+\omega_3+\omega_5+\omega_6+\omega_7+\omega_8)$$

$${}_1q = \frac{1}{6C_q}(\omega_3-\omega_4+\omega_5-\omega_6+\omega_7-\omega_8)$$

$${}_1r = \frac{1}{6C_r}(\omega_2-\omega_4+\omega_5+\omega_6-\omega_7-\omega_8).$$

Error detectors:

Roll axis ${}_1E_2 = {}_1E_3 = \frac{1}{6C_p}(2\omega_2+2\omega_3-\omega_5-\omega_6-\omega_7-\omega_8)$

${}_1E_5 = {}_1E_8 = \ldots$ etc.

Pitch axis ${}_1E_3 = {}_1E_4 = \frac{1}{6C_q}(2\omega_3-2\omega_4-\omega_5+\omega_6-\omega_7+\omega_8)$

${}_1E_5 = {}_1E_6 = \ldots$ etc.

Yaw axis ${}_1E_2 = {}_1E_4 = \frac{1}{6C_r}(2\omega_2-2\omega_4-\omega_5-\omega_6+\omega_7+\omega_8)$

${}_1E_5 = {}_1E_7 = \ldots$ etc.

In all the above cases the error detection threshold is $2\delta G/C_p$, $2\delta G/C_q$, $2\delta G/C_r$ for roll, pitch and yaw axes respectively.

NOTE: The error detection algorithms are different for each control axis.

### A.3. After Second Failure (say $\omega_2$)

Outputs:

$$_{12}p = \frac{1}{4C_p}(\omega_5+\omega_6+\omega_7+\omega_8)$$

$$_{12}q = {}_1q = \frac{1}{6C_q}(\omega_3-\omega_4+\omega_5-\omega_6+\omega_7-\omega_8).$$

Since for this axis $\omega_1$ and $\omega_2$ form a single estimate therefore a failure of $\omega_1$ has already disconnected the $\omega_2$ output.

$$_{12}r = \frac{1}{4C_r}(\omega_5+\omega_6-\omega_7-\omega_8).$$

## APPENDIX B

## Eight Gyro Pyramid Set B Consolidation Algorithms

### B.1. No failures

$$p = \frac{1}{8C_p}\{\omega_1+\omega_2+\omega_3+\omega_4+\omega_5+\omega_6+\omega_7+\omega_8\} \tag{B-1}$$

$$q = \frac{1}{8C_q}\{\omega_1-\omega_2+\omega_3-\omega_4+\omega_5-\omega_6+\omega_7-\omega_8\} \tag{B-2}$$

$$r = \frac{1}{8C_r}\{\omega_1+\omega_2-\omega_3-\omega_4+\omega_5+\omega_6-\omega_7-\omega_8\}. \tag{B-3}$$

### B.2. After first failure (say $\omega_1$)

$$_1p = \frac{1}{12C_p}\{2\omega_2+2\omega_3+\omega_4+2\omega_5+2\omega_6+2\omega_7+\omega_8\} \tag{B-4}$$

$$_1q = \frac{1}{12C_q}\{-\omega_2+2\omega_3-2\omega_4+2\omega_5-\omega_6+2\omega_7-2\omega_8\} \tag{B-5}$$

$$_1r = \frac{1}{12C_r}\{2\omega_2-\omega_3-2\omega_4+2\omega_5+2\omega_6-\omega_7-2\omega_8\}. \tag{B-6}$$

### B.3. After second failure

*B.3.1. Parallel failure (say $\omega_1$ and $\omega_5$)*

$$_{15}p = \frac{1}{4C_p}\{\omega_2+\omega_3+\omega_6+\omega_7\} \tag{B-7}$$

$$_{15}q = \frac{1}{4C_q}\{\omega_3-\omega_4+\omega_7-\omega_8\} \tag{B-8}$$

$$_{15}r = \frac{1}{4C_r}\{\omega_2-\omega_4+\omega_6-\omega_8\}. \tag{B-9}$$

*B.3.2. Non-parallel failure leaving four valid estimates in roll (say $\omega_1$ and $\omega_2$)*

$$_{12}p = \frac{1}{8C_p}\{\omega_3+\omega_4+2\omega_5+2\omega_6+\omega_7+\omega_8\} \tag{B-10}$$

$$_{12}q = \frac{1}{10C_q}\{2\omega_3 - 2\omega_4 + \omega_5 - \omega_6 + 2\omega_7 - 2\omega_8\}^* \tag{B-11}$$

$$_{12}r = \frac{1}{8C_r}\{-\omega_3 - \omega_4 + 2\omega_5 + 2\omega_6 - \omega_7 - \omega_8\} \tag{B-12}$$

*B.3.3. Non-parallel failures leaving five valid estimates in roll (say $\omega_1$ and $\omega_4$)*

$$_{14}p = \frac{1}{10_p}(2\omega_2 + 2\omega_3 + \omega_5 + 2\omega_6 + 2\omega_7 + \omega_8) \tag{B-13}$$

$$_{14}q = \frac{1}{8C_q}(-\omega_2 + \omega_3 + 2\omega_5 - \omega_6 + \omega_7 - 2\omega_8) \tag{B-14}$$

$$_{14}r = \frac{1}{8C_r}(\omega_2 - \omega_3 + 2\omega_5 + \omega_6 - \omega_7 - 2\omega_8). \tag{B-15}$$

## APPENDIX C

### Eight Gyro Pyramid Set B Failure Transients†

### C.1. First Failure

*C.1.1. Pre-Detection Transient.* Consider the situation where the errors in the correctly functioning gyros are such that $E_1 = +8\delta G$. This occurs when the error in $\omega_1$ is $+\delta G$ and the errors in the other gyros, $\omega_2$ to $\omega_8$ are $-\delta G$, $-\delta G$, $+\delta G$, $+\delta G$, $-\delta G$, $-\delta G$, $+\delta G$ respectively. If now $\omega_1$ fails such that the error in its output becomes negative, $E_1$ will be less than $-8\delta G$ when the error in $\omega_1$ is more negative than $-7\delta G$. At this point $\omega_1$ will be cut out. Hence the change in the error in $\omega_1$ is from $+\delta G$ to $-7\delta G$, i.e. $8\delta G$. This represents the maximum change due to failure as defined in Section 2.2. Substituting into the output algorithms (B-1), (B-2) or (B-3), gives a maximum pre-detection transient of $\delta G/C_p$ in all axes. The pre-detection transient can be smaller than this; if in the example above the $\omega_1$ failure had been in the positive direction a zero predetection transient would have been experienced if the error in $\omega_5$ was $-\delta G$, since $E_9$ would have indicated a failure immediately the error in $\omega_1$ exceeded $+\delta G$.

*C.1.2. Switch-Over Transient.* Differencing equations (B-1) and (B-4) of Appendix B gives the pitch axis switch-over transient for a failure of gyro $\omega_1$.

$$p - {}_1p = \frac{1}{24C_p}(3\omega_1 - \omega_2 - \omega_3 + \omega_4 - \omega_5 - \omega_6 - \omega_7 + \omega_8).$$

An identical expression is produced for $(q - {}_1q)$ and $(r - {}_1r)$. Using the error detection algorithms for $\omega_1$, i.e.

$$E_1 = 2\omega_1 - \omega_2 - \omega_3 + \omega_4 - \omega_6 - \omega_7 + \omega_8$$

the above can be rewritten as

$$p - {}_1p = \frac{1}{24C_p}(E_1 + \omega_1 - \omega_5).$$

Now for a failure of $\omega_1$ in a negative direction as derived in Section C.1.1 above, the maximum value of $\omega_1$ is $-7\delta G$ when $E_1 = -8\delta G$. $\omega_5$ is not represented in $E_1$ and can therefore be chosen to add to the magnitude

---

* Based on five valid estimates.

† Derived for $C_p = C_q = C_r$. In other cases replace $C_p$ by $C_q$, $C_r$ and select the expression relevant to the particular axis.

Therefore the maximum (and also the minimum, since $\omega_5$ can only be disconnected when ${}_1E_5$ exceeds $10\delta G$) switch-over transient in the parallel failure case is $5\delta G/6C_p$ in all three axes.

Following failures of $\omega_1$ and then $\omega_2$, the roll switch-over transient is given by $({}_1p - {}_{12}p)$. From (B-4) and (B-10) of Appendix B

$$
\begin{aligned}
{}_1p - {}_{12}p &= \frac{1}{24C_p}(4\omega_2 + \omega_3 - \omega_4 - 2\omega_5 - 2\omega_6 + \omega_7 - \omega_8) \\
&= \frac{1}{24C_p}(-{}_1E_2 + 2\omega_2 - 2\omega_6).
\end{aligned}
$$

At disconnect the maximum values of ${}_1E_2$ and $\omega_2$ are as derived in Section C.1.1 above and are $-8\delta G$ and $7\delta G$ respectively. Since $\omega_6$ is not contained in ${}_1E_2$ it can be chosen to increase the transient. Hence the maximum value is

$$
\frac{1}{24C_p}(8\delta G + 2(7\delta G) + 2(\delta G)) = \frac{\delta G}{C_p}.
$$

As for the first failure $\omega_2$ and $-{}_1E_2$ must have the same sign hence the minimum transient occurs when $(\omega_2 - \omega_6)$ equals $2\delta G$, and $-{}_1E_2$ must be $8\delta G$ hence the minimum transient for this case is $\delta G/2C_p$.

The third class of failure is typified by the switch over transient in roll following failures of $\omega_1$ and then $\omega_4$. In this case the transient is $({}_1p - {}_{14}p)$. From (B-4) and (B-13) of Appendix B

$$
\begin{aligned}
{}_1p - {}_{14}p &= \frac{1}{60C_p}(-2\omega_2 - 2\omega_3 + 5\omega_4 + 4\omega_5 - 2\omega_6 - 2\omega_7 - \omega_8) \\
&= \frac{1}{60C_p}(2({}_1E_4) + \omega_4 - \omega_8).
\end{aligned}
$$

Using the method of Section C.1.1 the values of ${}_1E_4$ and $\omega_4$ at switch over will be $8\delta G$ and $7\delta G$ respectively giving a switch-over transient for this case of

$$
\begin{aligned}
{}_1p - {}_{14}p &= \frac{1}{60C_p}(2(8\delta G) + 7\delta G + \delta G) \\
&= \frac{2\delta G}{5C_p}.
\end{aligned}
$$

This is not the 'maximum' since as explained in Section 6.2.1 it is possible for ${}_1E_4$ to be equal to $12\delta G$ when $\omega_4$ is $+3\delta G$ and $\omega_8$ is $+\delta G$. The transient then is

$$
{}_1p - {}_{14}p = \frac{1}{60C_p}(2(12\delta G) + 3\delta G - \delta G) = \frac{13\delta G}{30C_p}.
$$

This is the 'maximum' switch-over transient for this failure case. The minimum switch-over transient occurs as above when ${}_1E_4$ is $+8\delta G$ and $(\omega_4 - \omega_8)$ is $+2\delta G$. Hence the minimum is $3\delta G/10C_p$.

Of all the second failure cases the largest switch over transient is that of a non-parallel pair (e.g. $\omega_1$ and $\omega_2$) which can give a 'maximum' switch-over transient of $\delta G/C_p$. The 'minimum' switch-over transient occurs for the other type of non-parallel pair failure (e.g. $\omega_1$ and $\omega_4$) and is $3\delta G/10C_p$.

TABLE 1

**Failure transients for Twelve Gyro Orthogonal Arrangement**

| | First failure | | Second failure | |
|---|---|---|---|---|
| | Pre-detection | Switch-over | Pre-detection | Switch-over |
| Maximum | $\frac{7}{6}\delta G$ | $\frac{2}{3}\delta G$ | $\frac{5}{3}\delta G$ | $\delta G$ |
| Minimum | $\frac{1}{6}\delta G$ | $\frac{2}{3}\delta G$ | $\frac{1}{3}\delta G$ | $\delta G$ |

TABLE 2

**Maximum (Minimum) Failure Transients**

| Replace $C_p$ by $C_q$, $C_r$ for pitch, yaw axes respectively | First failure | | Second failure | |
|---|---|---|---|---|
| | Pre-detection | Switch-over | Pre-detection | Switch-over |
| 12 Gyro Orthogonal Arrangement | $\frac{7}{6}\delta G\left(\frac{1}{6}\delta G\right)$ | $\frac{2}{3}\delta G\left(\frac{2}{3}\delta G\right)$ | $\frac{5}{3}\delta G\left(\frac{1}{3}\delta G\right)$ | $\delta G(\delta G)$ |
| Pyramid Set A algorithms | $\frac{7}{6}\frac{\delta G}{C_p}\left(\frac{1}{6}\frac{\delta G}{C_p}\right)$ | $\frac{2}{3}\frac{\delta G}{C_p}\left(\frac{2}{3}\frac{\delta G}{C_p}\right)$ | $\frac{5}{3}\frac{\delta G}{C_p}\left(\frac{1}{3}\frac{\delta G}{C_p}\right)$ | $\frac{\delta G}{C_p}\left(\frac{\delta G}{C_p}\right)$ |
| Pyramid Set B algorithms | $\frac{\delta G}{C_p}(0{\cdot}0)$ | $\frac{2}{3}\frac{\delta G}{C_p}\left(\frac{1}{3}\frac{\delta G}{C_p}\right)$ | $\frac{3}{2}\frac{\delta G}{C_p}(0{\cdot}0)$ | $\frac{\delta G}{C_p}\left(\frac{3\delta G}{10C_p}\right)$ |
| Pyramid Set C algorithms | $\frac{\delta G}{C_p}(0{\cdot}0)$ | $\frac{2}{3}\frac{\delta G}{C_p}\left(\frac{1}{3}\frac{\delta G}{C_p}\right)$ | $\frac{5}{3}\frac{\delta G}{C_p}(0{\cdot}0)$ | $\frac{\delta G}{C_p}\left(\frac{3\delta G}{10C_p}\right)$ |

TABLE 3

**Ratio of Maximum (Minimum) Eight Gyro Pyramid to Conventional Twelve Gyro System Failure Transients**

| $C_p = C_q = C_r = \sqrt{\frac{I}{3}}$ | First failure | | Second failure | |
|---|---|---|---|---|
| | Pre-detection | Switch-over | Pre-detection | Switch-over |
| Twelve Gyro Orthogonal Arrangement | 1 (1) | 1 (1) | 1 (1) | 1 (1) |
| Pyramid Set A algorithms | 1·73 (1·73) | 1·73 (1·73) | 1·73 (1·73) | 1·73 (1·73) |
| Pyramid Set B algorithms | 1·48 (0·0) | 1·73 (0·86) | 1·56 (0·0) | 1·73 (0·52) |
| Pyramid Set C algorithms | 1·48 (0·0) | 1·73 (0·86) | 1·73 (0·0) | 1·73 (0·52) |

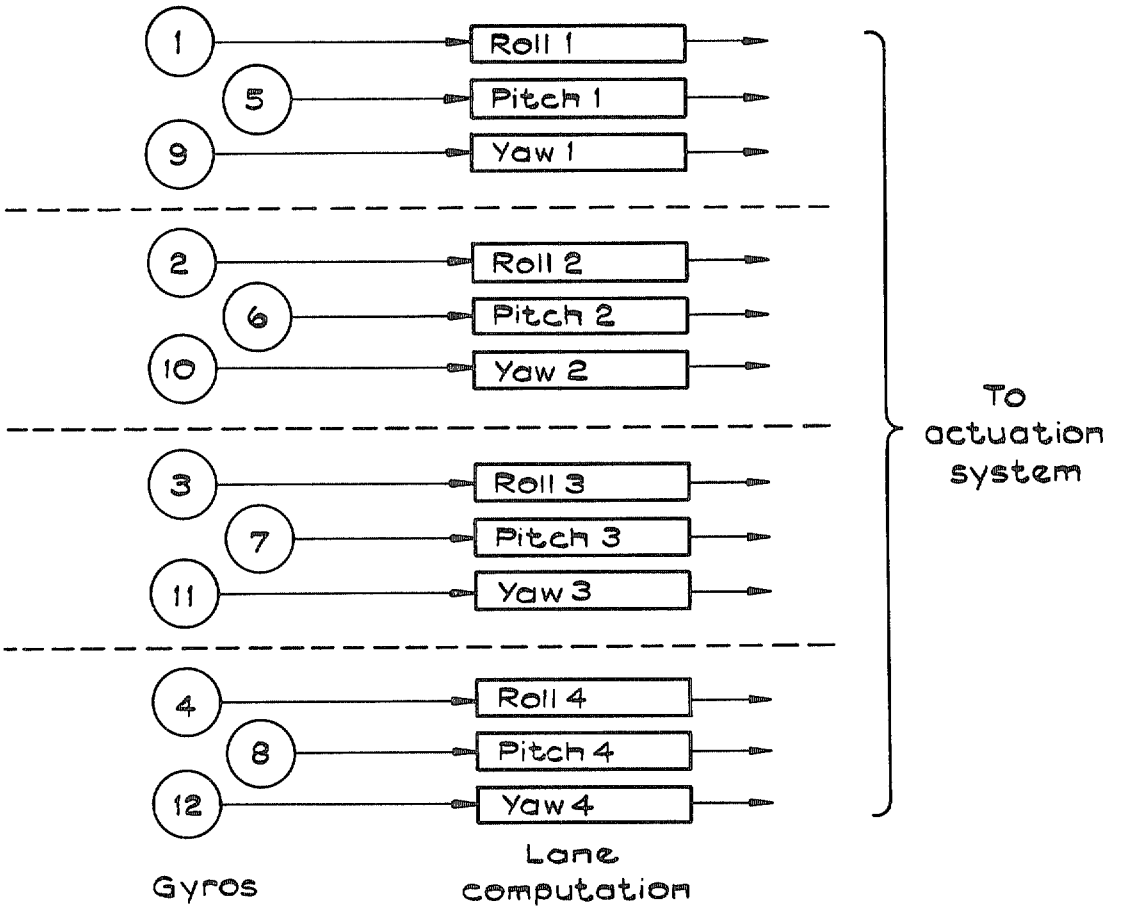


FIG. 1. A quadruplex flight control system.

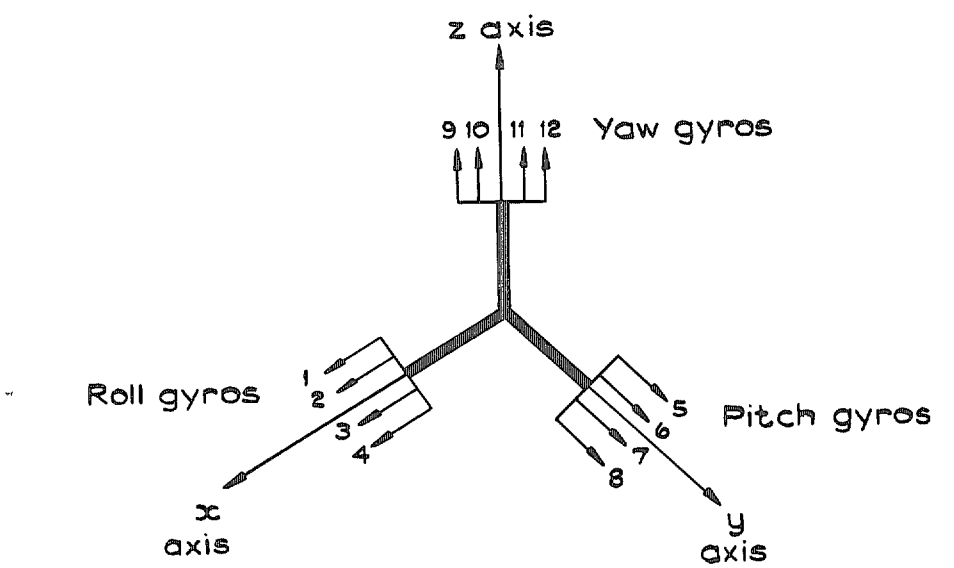


FIG. 2. Twelve gyro orthogonal arrangement.

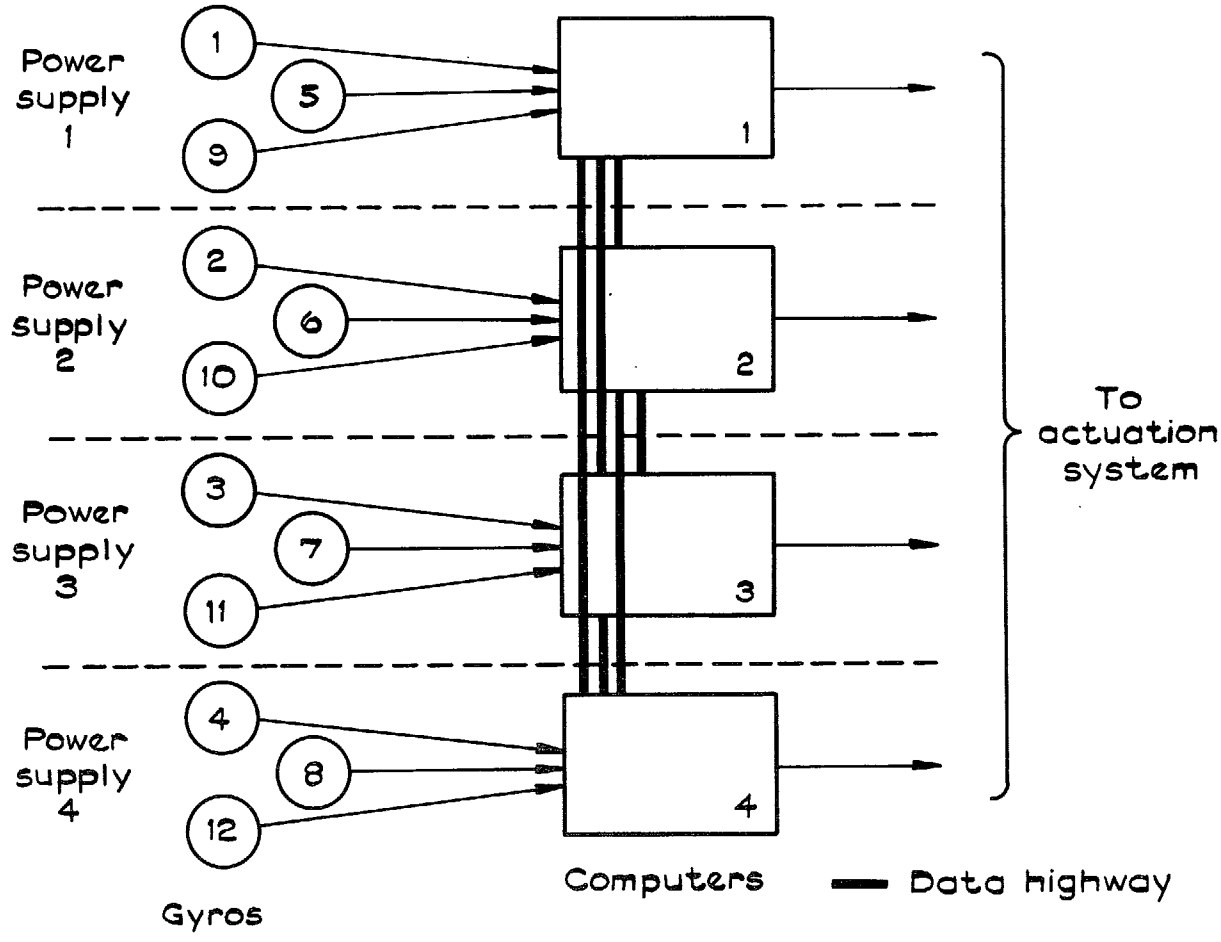


FIG. 3. Quadruplex system with interlane consolidation.

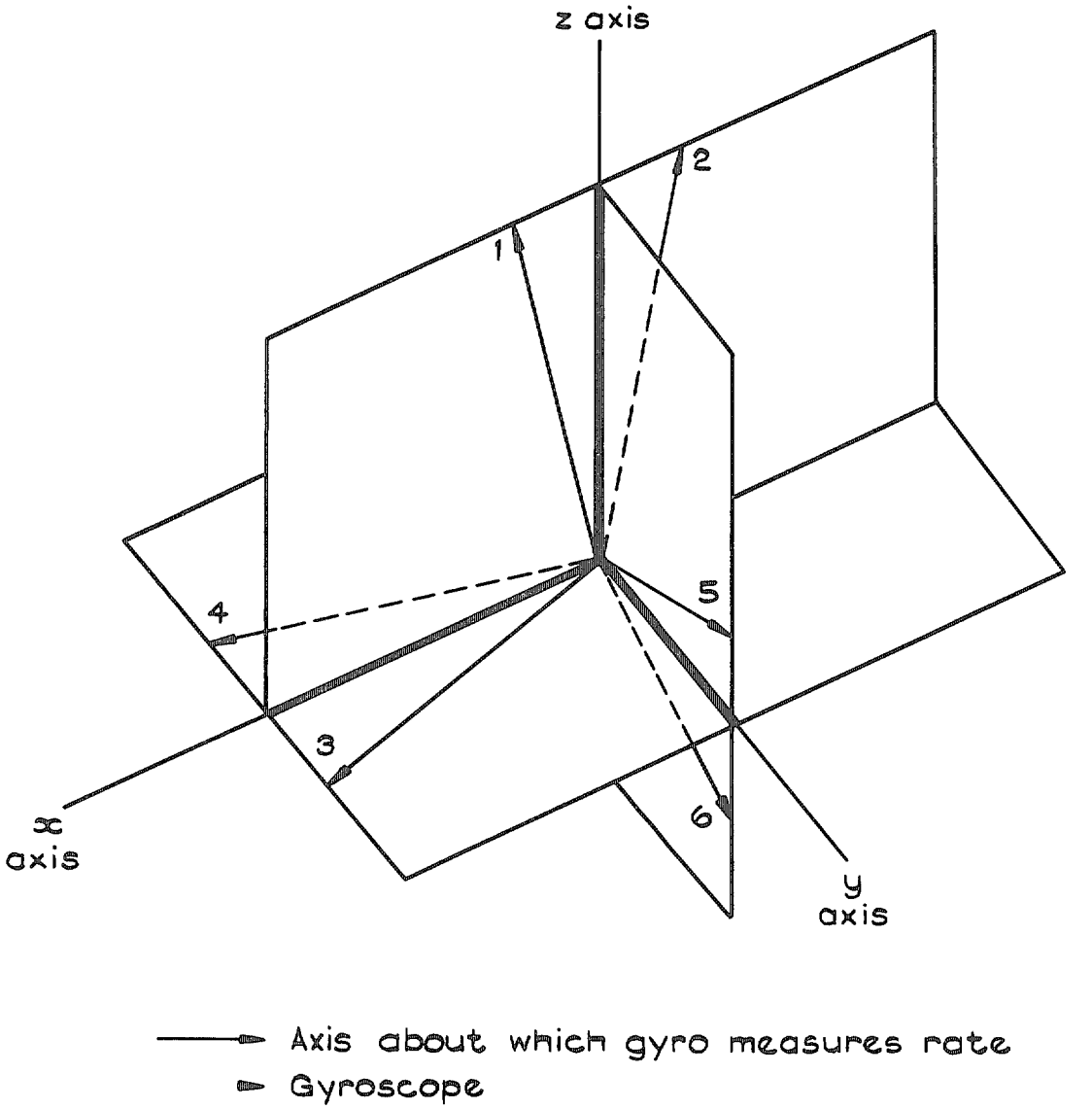


FIG. 4. A Six gyro 'two defect survival' arrangement.

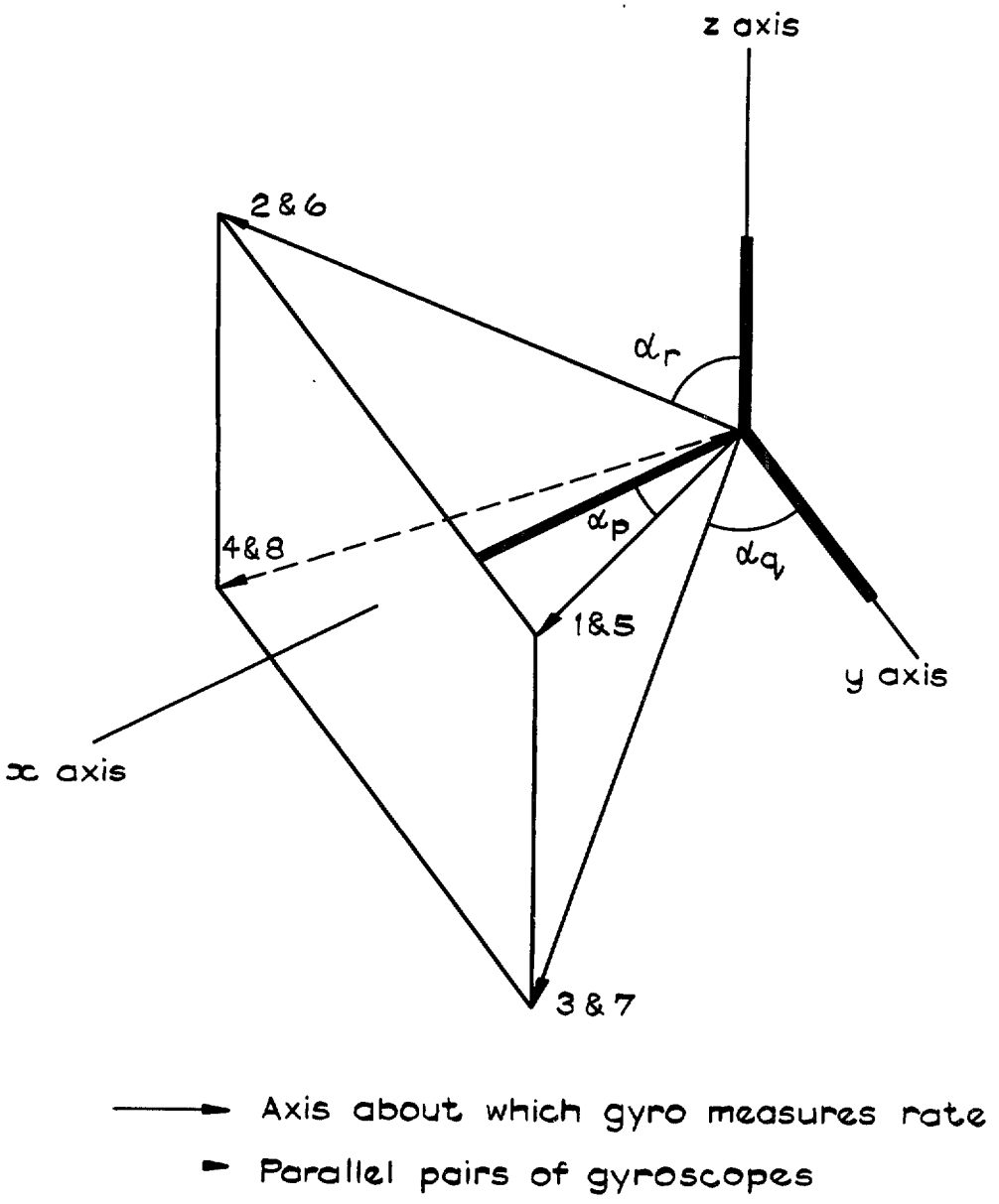


FIG. 5. Eight gyro pyramid arrangement.

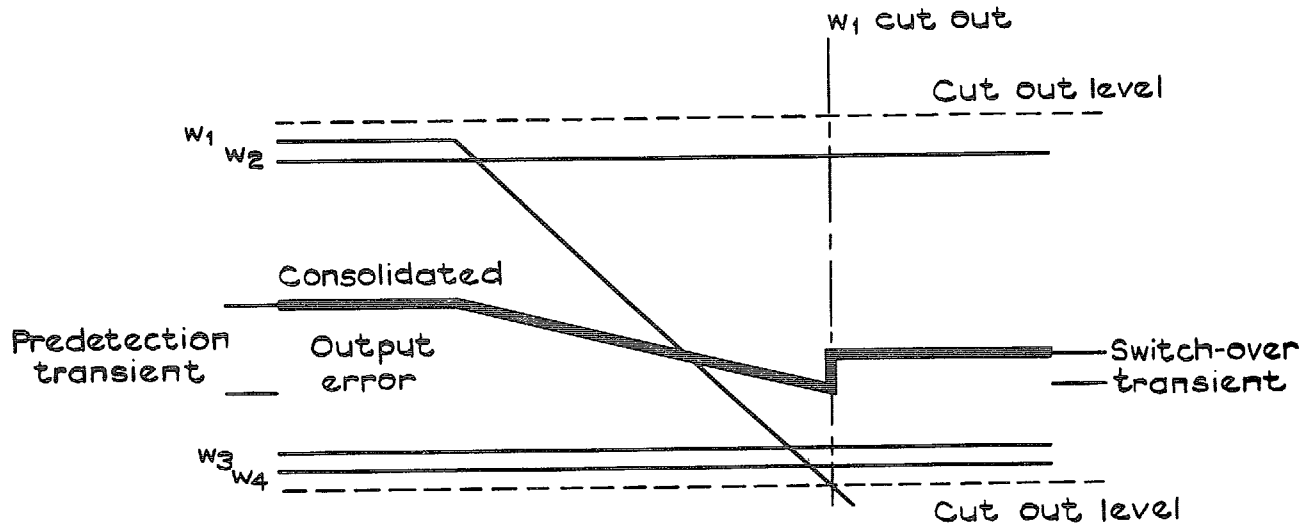


FIG. 6. Predetection and switch-over failure transients.

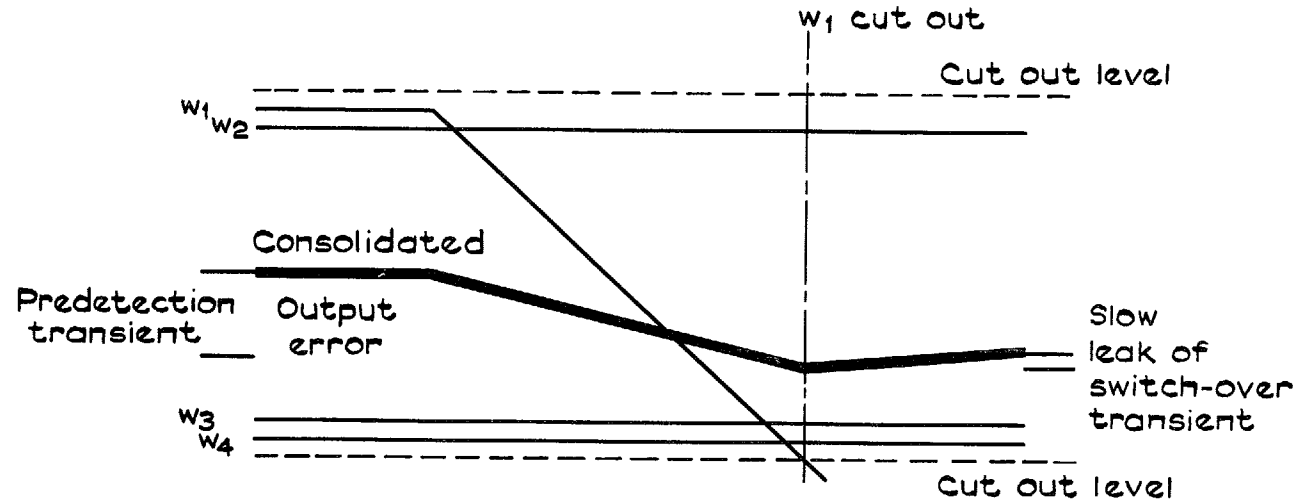


FIG. 7a. Switch-over transient suppression—'slow' failure.



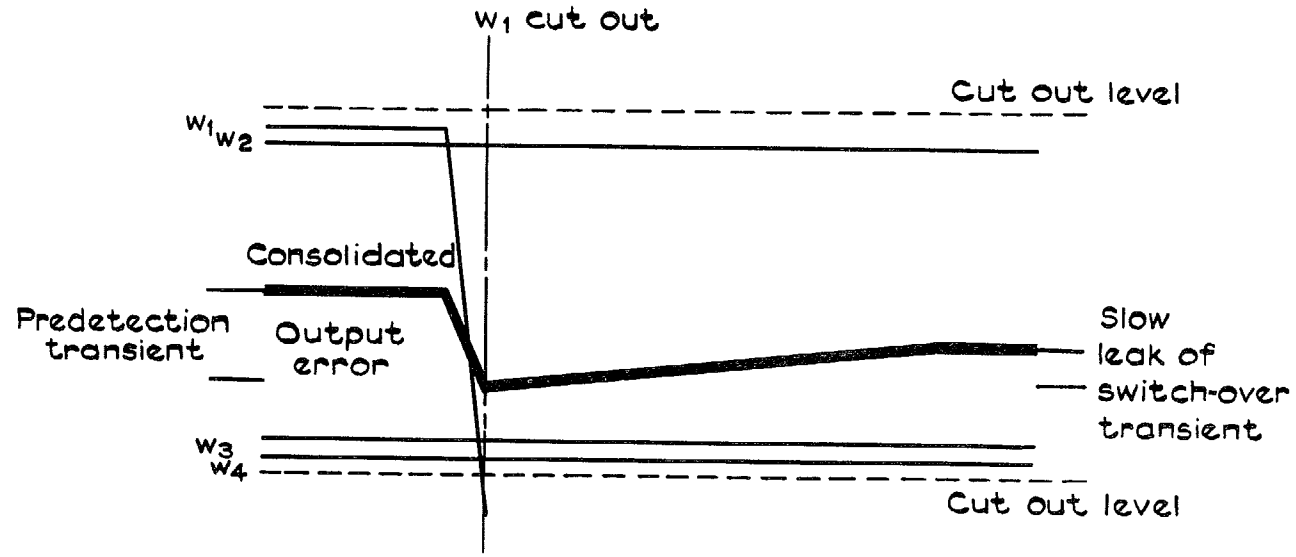


FIG. 7b. Switch-over transient suppression—'rapid' failure.

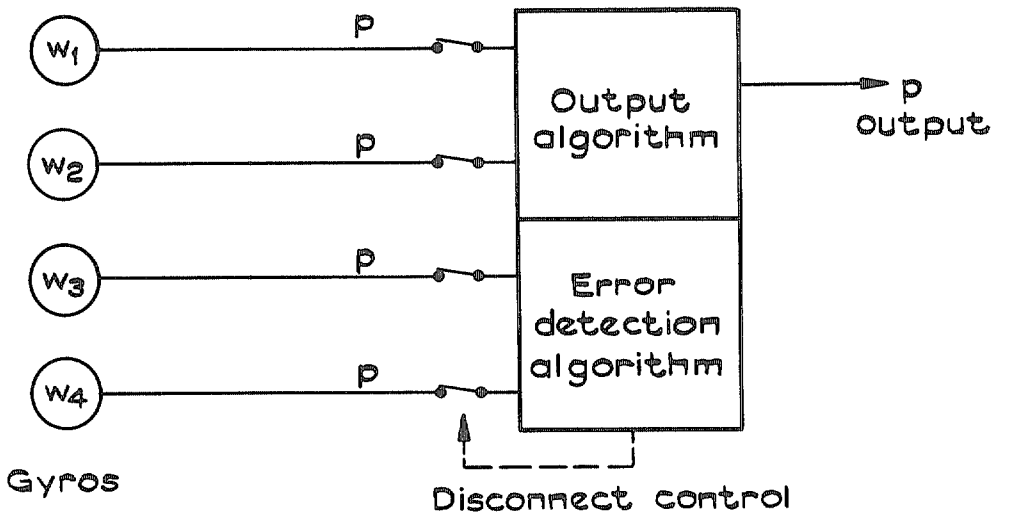


FIG. 8a. Twelve gyro orthogonal arrangement—roll axis algorithm configuration.

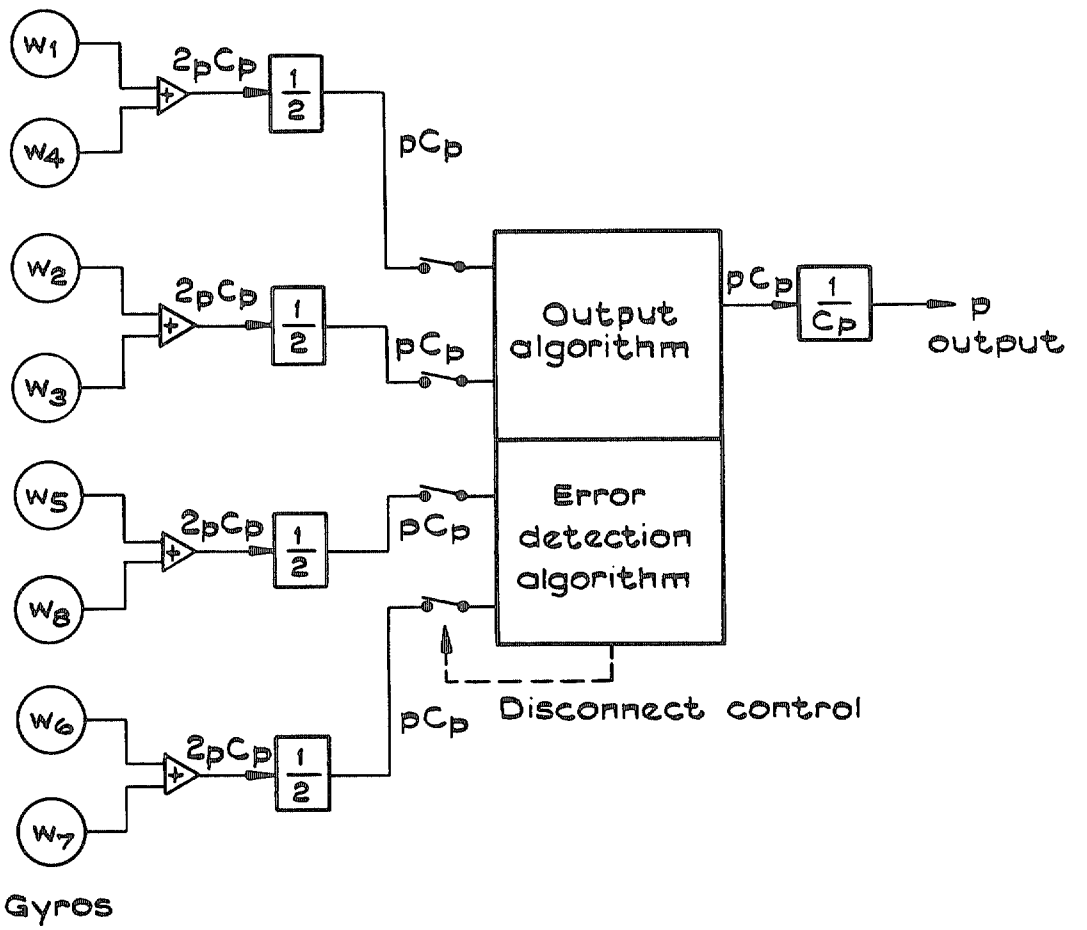


FIG. 8b. Pyramid set A arrangement—roll axis algorithm configuration.

FIG. 9a. Non-viable eight gyro—four computer interface arrangement.

FIG. 9b. Viable eight gyro–four computer interface arrangement.

Printed in England for Her Majesty's Stationery Office by J. W. Arrowsmith Ltd., Bristol BS3 2NT
Dd. 587484 K.4. 12/77.

HER MAJESTY'S STATIONERY OFFICE

*Government Bookshops*

49 High Holborn, London WC1V 6HB
13a Castle Street, Edinburgh EH2 3AR
41 The Hayes, Cardiff CF1 1JW
Brazennose Street, Manchester M60 8AS
Southey House, Wine Street, Bristol BS1 2BQ
258 Broad Street, Birmingham B1 2HE
80 Chichester Street, Belfast BT1 4JY

*Government Publications are also available through booksellers*

R. & M. No. 3808

ISBN 0 11 471141 0